

UC San Diego

UC San Diego Electronic Theses and Dissertations

Title

Protease-Based Magnetic Sensor for Rapid Detection of Candidemia

Permalink

<https://escholarship.org/uc/item/1wg48381>

Author

Jain, Sonal

Publication Date

2017

Peer reviewed|Thesis/dissertation

UNIVERSITY OF CALIFORNIA, SAN DIEGO

Protease-Based Magnetic Sensor for Rapid Detection of Candidemia

A Thesis submitted in partial satisfaction of the requirements
for the degree Master of Science

in

Bioengineering

by

Sonal Jain

Committee in charge:

Professor Drew A. Hall, Chair
Professor Anthony J. O'Donoghue, Co-Chair
Professor Michael J. Heller, Co-Chair
Professor Geert Schmid-Schonbein

2017

Copyright

Sonal Jain, 2017

All rights reserved.

The Thesis of Sonal Jain is approved and it is acceptable in quality and form for publication on microfilm and electronically:

Co-Chair

Co-Chair

Chair

University of California, San Diego

2017

TABLE OF CONTENTS

Signature Page.....	iii
Table of Contents.....	iv
List of Figures.....	vi
List of Tables.....	viii
Acknowledgements.....	ix
Abstract of Thesis.....	xi
Chapter 1: Introduction.....	1
1.1 Research Motivation.....	1
1.2 Background.....	2
1.3 Thesis Objective.....	5
1.4 Thesis Organization.....	6
Chapter 2: Surface Functionalization.....	7
2.1 Introduction.....	7
2.2 Immobilization Scheme 1: Amide Bond Formation.....	9
2.2.1 Introduction.....	9
2.2.2 Materials and Methods.....	10
2.2.3 Results and Discussion.....	12
2.3 Immobilization Scheme 2: Cysteine-Maleimide Coupling.....	15
2.3.1 Underlying Chemistry.....	15
2.3.2. Materials and Methods.....	16
2.3.3 Results and Discussion.....	19

Chapter 3: Protease Assays.....	21
3.1 Protease Biochemistry.....	21
3.2 Optical Digestion Assays.....	22
3.2.1 Introduction.....	22
3.2.2 Methods and Results.....	23
3.3 GMR Sensors.....	29
3.3.1 Introduction.....	29
3.3.2 Chip Fabrication and Functionalization.....	31
3.3.3 Analysis and Measurement Setup.....	35
3.3.4 Results and Discussion.....	38
Chapter 4: Conclusion.....	43
4.1 Summary.....	43
4.2 Future Directions.....	45
References.....	47

LIST OF FIGURES

Figure 2. 1: Illustration of the two custom designed peptides.....	8
Figure 2.2: Cleavage of fluorescent peptide.....	9
Figure 2.3: Carboxyl-amine crosslinking chemistry via EDC.....	10
Figure 2.4: Schematic representation of the optimized surface modification and peptide immobilization strategy.....	11
Figure 2.5: Fluorescent intensity data for 1 μ M peptide labeling on APTES treated plates.....	13
Figure 2.6: Comparison of peptide labeling between APTES treated and Covalink plates.....	14
Figure 2.7: Reaction scheme from thiol coupling between maleimide and cysteine...	15
Figure 2.8: Schematic for peptide immobilization on maleimide-activated polystyrene plates.....	17
Figure 2.9: Reaction chemistry between maleimide-activated BSA and my peptide...	18
Figure 2.10: Fluorescent readings from assay to quantify peptide attachment on pre maleimide-activated plates.....	19
Figure 2.11: Fluorescent readings from assay to optimize concentration of BSA-maleimide required for robust attachment of the peptide.....	20
Figure 3.1: Curves representing RFU values for cleavage reaction between the fluorescently labelled peptide and Sap6 and papain.....	23
Figure 3.2: Schematic illustrating the steps involved in setting up a digestion assay after the peptide is immobilized.....	24
Figure 3.3: Reaction wells setup for time-dependent digestion of peptide with 5.69 μ M papain.....	25
Figure 3.4: Reduction curve for time-dependent digestion of peptide with 5.69 μ M papain.....	25

Figure 3.5: Setup of experiment to verify cleavage of peptide.....	26
Figure 3.6: Plot of RFU values vs the level of peptide assembly at which protease was added.....	27
Figure 3.7: Plot of RFU values vs concentration of BSA-maleimide.	28
Figure 3.8: Illustration showing the GMR sensor chip	30
Figure 3.9: Measurement setup showing 50nm streptavidin coated superparamagnetic nanoparticles (MNPs).....	31
Figure 3.10: Transfer curve of a GMR SV sensor with the inset showing a photograph of the 16-pin sensor die.....	32
Figure 3.11: Reaction well showing the fabricated tygon tube well attached via epoxy on the chip.....	34
Figure 3.12: Measurement setup showing the readout circuitry, the Helmholtz coils, and the power amplifier.....	35
Figure 3.13: LabVIEW user interface showing the sensor grid.....	36
Figure 3.14: Screenshot of measurement data from pilot study ran to test BSA functionalization.....	37
Figure 3.15: Data readout of real-time binding and release of MNPs from the sensor on chip 0802.....	39
Figure 3.16: Bar plots comparing the loading and release of 1 μm MNPs after digestion with papain.....	41

LIST OF TABLES

Table 3:1: Concentrations of the BSA samples used to functionalize the sensors.....	34
---	----

ACKNOWLEDGEMENTS

My deepest gratitude goes to my two advisors, Drew A. Hall and Anthony J. O'Donoghue for seeing the potential in me and taking me under their wings. They have been outstanding mentors and the experience I hold of working with them is invaluable to me. From the first day, they have been extremely approachable and available. Their constant back-and-forth feedback was extremely helpful and really showed me the significance of critically analyzing each experiment I performed. Their enthusiasm for science is an inspiration to me and I hope I can be half as good a role model as they have proved for me.

Next, I would like to thank my co-chair Michael J. Heller for his support and feedback to my project. His passion for teaching and research is extremely infectious which was evident from his course, that I had the opportunity to take. I am truly grateful to have had the chance to have him as my co-chair.

I am also immensely grateful for Professor Geert Schmid-Schonbein for agreeing to be on my committee. His extreme willingness to meet with me and learn about my project was very motivating for me. I aspire to be a scientist and researcher like him someday.

Next, I would like to thank Clarissa Nobile and her research group for providing us with the fluorescent substrate we used in this study as well as the protease. Their work on identifying the peptide substrates and proteases secreted by *C. albicans* has been consulted innumerable times throughout this research.

I am also grateful to all the lab members of both the groups that I had the opportunity to work and interact with. First and foremost, I would like to thank Venkatesh for his tremendous help in the earlier stages of this project. I would not have been able to carry out my assays with so much ease and comfort if he had not been there to teach me the basic principles and procedures. I am also thankful to Xiahan and Iric for teaching me how to use the GMR sensors and take measurements on them in the downstairs lab. Their constant help and advice on the sensors was extremely valuable for me.

I would like to thank my brother, Praful, my sister-in-law, Sonam, and my boyfriend, Vinnu, for their unconditional love and support, and for always being there when I needed encouragement. Lastly, I cannot be more thankful to my mother, Ina, for her constant faith in me and for always encouraging me to become a hard-working and stronger individual, this thesis is dedicated to her.

ABSTRACT OF THE THESIS

Protease-Based Magnetic Sensor for Rapid Detection of Candidemia

by

Sonal Jain

Master of Science in Bioengineering

University of California, San Diego, 2017

Professor Drew A. Hall, Chair
Professor Anthony J. O'Donoghue, Co-Chair
Professor Michael J. Heller, Co-Chair

We are developing a rapid, point-of-care (POC) test for detection of Candidemia using giant magnetoresistive (GMR) biosensors. Candidemia is a fungal infection caused by the overgrowth of a yeast called *Candida albicans*. It is the 4th leading cause

of bloodstream infections in hospitalized patients in the U.S. and severely affects immunocompromised individuals. Candidemia can be fatal if not treated rapidly and is often only detected post-mortem. The current gold standard for its detection is a blood culture, which typically takes 3-5 days, wasting precious treatment time. Therefore rapid, unambiguous diagnosis is required to improve prognosis. This technology aims to detect a unique enzyme that is secreted by *C. albicans* during infection. This enzyme, Sap6, is a protease that can degrade a synthetic peptide. The POC test works by immobilizing magnetic nanoparticles onto the GMR biosensor via the peptide. Once peptide cleavage by Sap6 occurs, the magnetic nanoparticle is released away from the sensor surface. This change in the magnetic field of the GMR sensors is detected in real-time. We have demonstrated this proof-of-concept in a 96-well plate format using a fluorescent sensor. This assay immobilizes approximately 1.8 μg of peptide per well which can then be released by 13.34 μg of protease in 10 minutes at room temperature. We have translated the assay to the GMR biosensors and detected up to 60% reduction in signal within 60 minutes. We hope to optimize this technology by reducing the detection time and expand it further to test other diseases like cystic fibrosis.

CHAPTER 1: Introduction

1.1 Research Motivation

In recent years, there has been increasing interest in developing molecular tests for disease diagnostics, especially with the target of delivering less costly care in the patient's home. Current technologies for disease detection rely mainly on the presence of biomarkers, such as blood, urine, serum, and plasma in a sample. Biomarkers provide a dynamic approach to understanding the scope of a disease and have applications in screening, diagnosis, and prognosis. Infectious diseases are among the leading reasons for morbidity and death worldwide, especially in developing countries [1]. Many infectious diseases along with cancer have utilized techniques such as enzyme-linked immunosorbent assay (ELISA), polymerase chain reaction (PCR), immunofluorescence, and western blotting for disease detection [2]. Careful investigation of the validity of biomarkers is needed with respect to the stage of the disease. Sometimes these biomarkers are only detected once the disease has progressed to later stages due to their low abundance or inability to be screened by the detection mechanism, thus wasting precious treatment time. Early and timely detection of these biomarkers can be extremely crucial in improving molecular diagnosis platforms as they may lead to more cures and an increased chance of survival.

Traditional diagnostic methods are often bulky and require expensive instruments, such as an immunofluorescent reader, limiting their applications in low-resource settings. Therefore, there is an urgent need for a miniaturized, rapid and

portable point-of-care (POC) biosensor that can perform the entire diagnostic on a single chip in a timely manner. POC testing is at the forefront of biomedical innovation and its use has only increased in the last 40 years since it first came into use [3]. For example, glucose monitoring is one area of research that has been extensively studied via a POC approach and many glucose biosensors are being developed today that are faster and require smaller sample volumes as compared to their traditional laboratory counterparts [4]. Disease detection via POC biosensors offers many advantages over other diagnostic platforms as it has the potential to expedite treatment and reduce patient loss. In recent years, there has also been a growing trend in the use of smartphones as detection platforms [5]. Many biosensing technologies today are linked to a mobile application for continuous monitoring and quantification of different analytes levels. Biosensor diagnostic platforms, along with novel smartphone-based detection schemes are ultimately going to pave the way for personalized medicine, where the drug or treatment is catered to an individual's needs and genetic makeup.

1.2 Background

Candidemia is a fungal infection caused by the overgrowth of a yeast called *Candida albicans*. It is the 4th leading cause of bloodstream infections in hospitalized patients in the U.S. and severely affects immunocompromised individuals [6]. Candidemia can be fatal if not treated rapidly and is often only detected post-mortem. *C. albicans* can grow in a planktonic state or in a biofilm formation. As a biofilm, they organize themselves in drug resistant, and highly resilient-tightly packed communities attached to a solid surface, usually an implanted medical device or niches in the human

body. Sap5 and Sap6 are two aspartyl proteases that are secreted by *C. albicans* during biofilm formation. It has been shown that deletion of Sap5/6 specific genes on *in vivo* *C. albicans* causes a significant reduction in biofilm formation [7]. The standard treatment for individuals with Candida-infected medical implants is removal of the device. This requires surgical intervention and is only often treated after the infection has disseminated. Therefore, timely and rapid detection of these biofilm-specific proteases can provide a unique platform towards improving patient outcome.

The current gold standard for detection of candidemia is a blood culture, which requires large sample volume and typically takes 3-5 days to identify various *Candida* species. Additionally, nucleic acid- (NA) based detection is another approach clinicians have used to diagnose candida [8]. This is usually done via DNA microarray techniques where thousands of gene-specific probes are first immobilized on a solid substrate, and then exposed to a sample containing the complementary DNA sequences, which then leads to hybridization detected via an optical reporter label. Although this approach is rapid, due to the relatively small quantities of NAs, it is not very sensitive. PCR is often employed to amplify the signal, however the requirement to operate at three different temperatures can be expensive and hard to perform, particularly at the point-of-care. Therefore, techniques like lab-on-a-chip and microfluidics hold great promise, as they can enhance early detection and identification of the fungi. Currently, techniques based on dielectrophoresis (DEP) [9], digital microfluidics [10], and microchip PCR [11] are being explored for multiplex *Candida* detection with sensitivity as high as 1 CFU/mL. However, most of these techniques still require upto four to five hours for detection and can often be expensive to fabricate.

Enzymatic biosensors are an integral part of emerging technologies today in areas of clinical diagnostics and point-of-care analysis. They are widely used in healthcare with applications in blood glucose [12], uric acid [13], and opioid monitoring [14]. Enzyme biosensors utilize the selectivity and affinity of catalytic proteins, towards their target analytes. They can either detect the presence of a substrate, where an increase in signal is monitored; or detect presence of an inhibitor, in which case the decrease in signal is quantified. Significant advancements have been made in the field of enzymatic biosensors by exploiting genetically engineered enzymes [15] and using techniques such as Biocomputing [16]. However, challenges still exist to find optimal solutions that incorporate parameters like wide dynamic range, low limit of detection (LLD), and high sensitivity. This can be achieved by using novel approaches for detection and transduction of signal.

Magnetic sensor nanotechnologies hold great potential in biomedical applications, as they can improve the LLD due to negligible magnetic background signals present in biological samples. Magnetic nanoparticles (MNPs) have attracted a growing interest in developing biosensors due to their biocompatibility and high specificity. One of the first studies demonstrating use of MNPs was reported in 1998, where the researchers detected signals from MNPs using giant magnetoresistive (GMR) sensors [17]. GMR sensors operate isothermally and have simpler instrumentation, making them more suitable for POC applications. They are also cheap and can be easily made portable. Several groups worldwide are currently investigating magnetoresistive sensors and their applications in biological sensing [18-25]. From their use in DNA microarray [26] to a handheld laboratory stick [27], it is safe to say that this area of

research is on a growing trend. This work demonstrates their use as platforms for detecting presence of proteases via immobilization of a specific peptide sequence. The working of GMR sensors will be discussed more in detail in chapter 3.

1.3 Thesis Objective

Studying any aspect of disease progression requires understanding of specific biomarkers that are unique to the disease and its different stages. Therefore, techniques that enable rapid and early detection of these biomarkers hold the key to developing more sensitive biosensing platforms. The aim here is to establish a simple yet versatile approach to detect presence of proteases in a sample, via a highly specific immobilization chemistry for unique recognition.

This technology utilizes unique enzymes called proteases that can degrade a peptide sequence at a specific amino acid location with high specificity and selectivity. The aim of this study is to develop a rapid, POC *Candidemia* detection scheme using magnetic sensors that are sensitive to changes in their external magnetic field. This approach was first optimized by designing synthetic peptides labeled with a magnetic nanoparticle, that produces a demagnetizing field opposing the field from the GMR sensor. Optical assays on 96-well plates were carried out to establish a working protocol for immobilizing these peptides onto the magnetic sensor surface. The underlying principle is that when the protease in an infected sample detects a peptide that it wants to cut, the MNP is released from the peptide. As the MNP floats away from the surface of the sensor, the signal gradually drops and is detected in real time. Instead of

quantifying the total protein concentration, amplification of signal is detected by immobilizing thousands of peptides onto the sensor surface. The hope is to develop a protease-based biosensor that works isothermally, has high sensitivity and requires only 15-20 minutes to read out the results. By leveraging the unique property of the GMR sensors to detect changes in their external magnetic field, the overall aim to further expand this technology to detect other diseases such as Cystic Fibrosis (CF).

1.4 Thesis Organization

The rest of the thesis is presented as follows: Chapter 2 discusses labelled vs unlabeled detection as well as the various immobilization chemistries used to attach the peptide onto the plate surface. Chapter 3 provides an overview of proteases and how they can be used as biomarkers for detection. The initial optical assays carried out to establish an optimized working protocol for protease detection are also described. Next, a brief description of the GMR sensors and their working is given. Lastly, chapter 4 summarizes this work and includes all the future work for this study.

CHAPTER 2: Surface Functionalization

2.1 Introduction

Biosensors can be broadly classified into two categories: labeled and label free detection methods. In labeled techniques, a secondary molecule is tagged to the biomolecule of interest via one of the many following methods, namely, (1) fluorescent labeling [28], (2) quantum dot labeling [29], (3) electrochemically active probe [30], and (5) magnetic tag [31]. These labelling processes usually involve covalent binding through coupling chemistries. On the other hand, label-free techniques such as mass spectrometry [32], surface plasmon resonance [33], and microcantilevers [34] measure an intrinsic property of the biomolecule, such as mass, charge, size, or thermal reactivity. Overall, these approaches have a common aim of observing molecular binding events with high sensitivity to minute changes and producing a high signal-to-noise ratio.

The first step of the study here is to detect the immobilization of an 8-mer peptide sequence onto the sensor surface. All optimization studies for attachment and orientation of the substrate onto a solid surface were performed on 96-well plates in an ELISA format. For these optical assays, fluorescent and colorimetric labeling were used as the detection schemes and all readings were taken and analyzed on a microplate reader (SynergyTM HTX Multi-Mode Reader). The immobilization schemes studied and implemented are discussed in the sub-sections below. A series of covalent linkages form

highly specific and irreversible bonds that are stable at different temperatures and pH. Figure 2.1 illustrates the two peptides used in this study which contain the sequences cleavable by Sap6 as described in [35]. The authors in this study used mass spectrometry

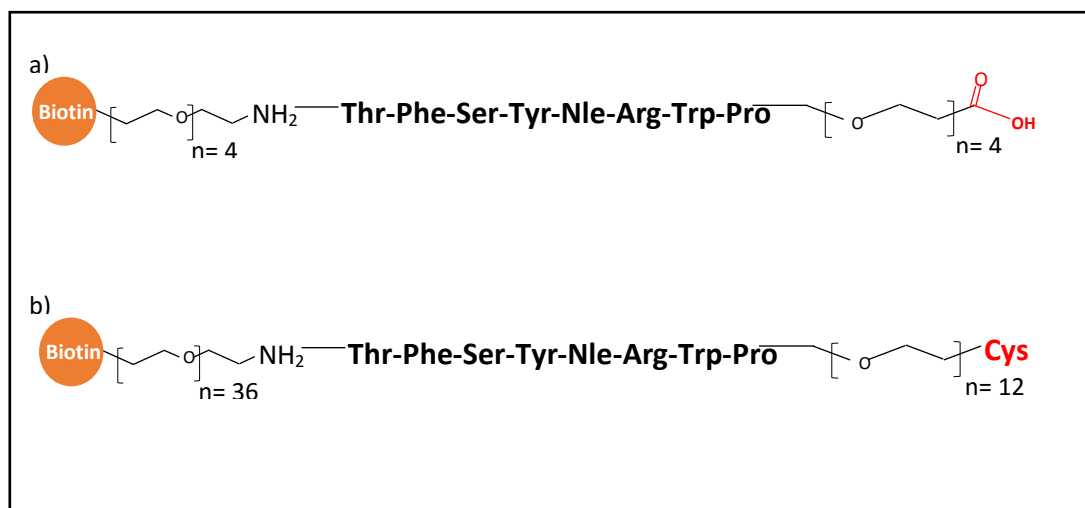


Figure 2.1: Illustration of the two custom designed peptides. The peptides share the same amino acid sequence however differ by the length of the PEG molecule used and their end groups: a) PEG4 on both ends and free carboxyl group on one end to form amide bond, and b) PEG36 closer to the biotin end and PEG12 closer to cysteine end.

(MS) to identify sequences cleaved in a peptide library by *C. albicans* biofilms. The sequence found to have the highest selectivity for Sap6 was TFSYnRWP, where lower case “n” corresponds to the non-natural amino acid, norleucine. Cleavage of this peptide was found to occur between tyrosine and norleucine at pH 5.0. Along with the peptide synthesized in Figure 2.1, a fluorogenic peptide substrate of the same sequence was also used to optimize working concentrations for cleavage by Sap6, as illustrated in Figure 2.2. The custom designed peptides also contain PEG linkers on both the ends to prevent steric hindrance from the streptavidin and hence rendering the cleavage site more accessible to the protease.

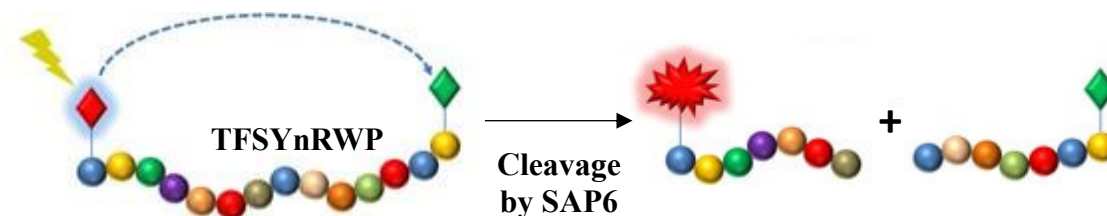


Figure 2.2: Cleavage of fluorescent peptide. On cleavage of the specific peptide sequence by the protease, the quencher and fluorophore are separated giving a large increase in fluorescence via FRET.

2.2 Immobilization Scheme 1: Amide bond formation

2.2.1 Introduction

Methods for immobilization of biomolecules, such as peptides and DNA to polystyrene surfaces are well established [36]. Every chemical modification or conjugation process involves formation of a covalent bond, via a reaction between two functional groups. Reactive crosslinking groups can include carboxylic acids, primary amines, thiols, and alcohols. A substrate containing the amino acid sequence TFSYnRWP, flanked on each end by a PEG linker as illustrated in Figure 2.1(a). was designed for cleavage by Sap6. There were no aspartic acid or glutamic acid residues in the peptide, and therefore the only available carboxylic acid was at the terminus. The end consisting of a free carboxyl group was covalently bound to amine groups on the plate via 1-ethyl-3-(3-dimethylaminopropyl) carbodiimide (EDC). Carbodiimide compounds are one of the most common and versatile molecules for labelling and crosslinking to carboxylic acids [37]. They are zero-length crosslinking agents as no additional chemical structure is introduced between the two reactive species during the formation of the covalent bond. The EDC reaction chemistry works by activating

carboxyl groups to immediately react with primary amines via amide bond formation (Fig. 2.3). This section covers the materials, methods, and optimization techniques implemented to test the chemistry used for immobilization of the synthetic peptide. A brief description is also provided for why this strategy did not work as well as hoped for the immobilization of the peptide and the alternative approach tested.

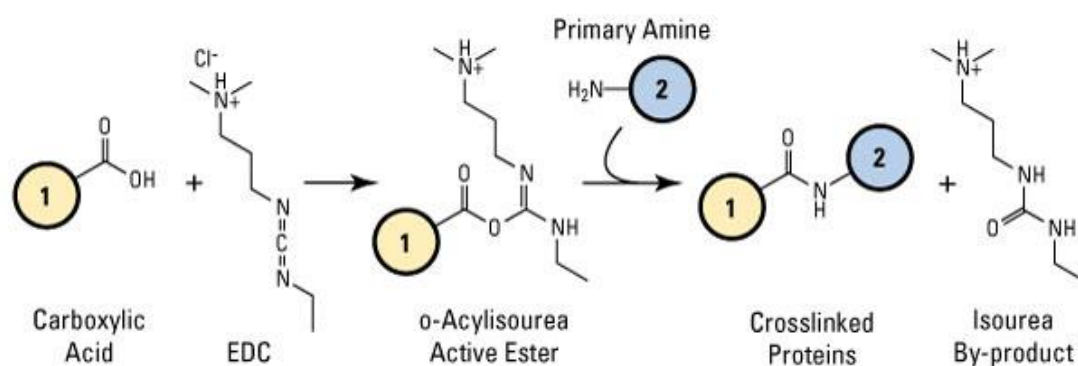


Figure 2.3: Carboxyl-amine crosslinking chemistry via EDC. Molecule 1 represents the synthetic peptide from figure 2.1a and molecule 2 is the surface of the amine functionalized polystyrene plates.

2.2.2 Materials and Methods

All reagents were purchased from Thermo Scientific and stored per the recommended conditions. 96-well black non-tissue culture treated polystyrene plates were used for the initial studies. The surface activation was done via 1% potassium hydroxide (KOH) to introduce hydroxyl groups. 3-aminopropyltriethoxysilane was then added to functionalize the surface with free primary amines. Figure 2.4 gives the schematic of the functionalization scheme and peptide immobilization. EDC chemistry

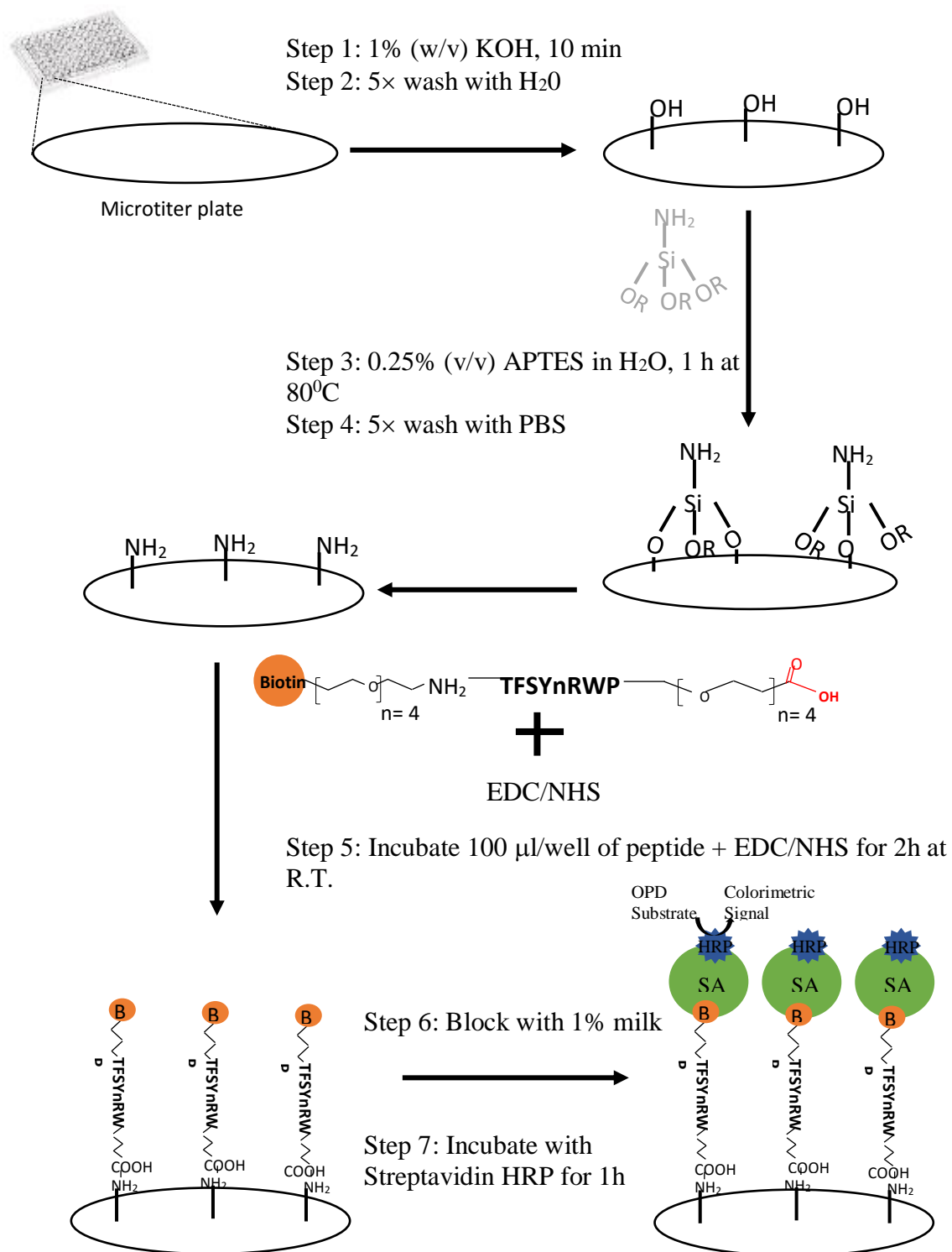


Figure 2.4: Schematic representation of the optimized surface modification and peptide immobilization strategy.

is known to perform best at in acidic conditions (pH 4.5-7.2) whereas the activation

buffer is known to perform best at acidic conditions (pH 4.5-7.2). Activation buffer containing 0.1M MES, 0.5M NaCl, pH 6.0 was prepared to perform step 5 in Figure 2.4. An additional blocking step using 1% milk was also added to avoid non-specific binding of streptavidin to the plate surface. Streptavidin conjugated with horse radish peroxidase (HRP) enzyme was used to measure the signal of the immobilized peptide. The streptavidin-HRP forms a covalent bond with the free biotin on the other end of the peptide, and generates a colorimetric signal when reacted with the HRP substrate: o-phenylenediamine dihydrochloride (OPD).

Subsequently, to minimize the conjugation steps, pre-amine activated plates from Thermo Scientific (Nunc Covalink NH™) that were functionalized with secondary amino groups were purchased. The conjugation steps performed were the same as KOH/APTES activation except that steps 1-4 were omitted and sulfo-NHS was used prior to EDC addition. All the steps were derived from the Thermo Scientific NUNC Covalink™ manual [38]. A 100 μ L/well NHS-peptide solution was first added to the plates followed by 50 μ L of the EDC solution. The entire mixture was incubated overnight and then washed 3 \times with Covabuffer (2M NaCl, 1% MgSO₄, 0.05% Tween 20 in 1 \times PBS) followed by blocking with 1% milk and detection via Streptavidin conjugated with a fluorescent dye with excitation/emission ~365/460 nm.

2.2.3 Results and Discussion

Extensive optimization studies were carried out on both the APTES treated plates as well as the commercial Covalink NH plates. Even though the EDC/NHS protocol is well documented in the literature and proven to be successful in forming an amide bond

between a carboxyl and an amine group, inconsistent labeling was achieved, perhaps due to the structure of the peptide. Several experiments were performed to test the robustness of the peptide attachment, however it was consistently found that in the presence of 0.01% Tween 20, most of the binding was being lost. Figure 2.5 shows the data generated from an experiment using 1 μM peptide on APTES treated plates. The peptide was incubated overnight and washed with the labeled chemical 3 \times on day 2. It

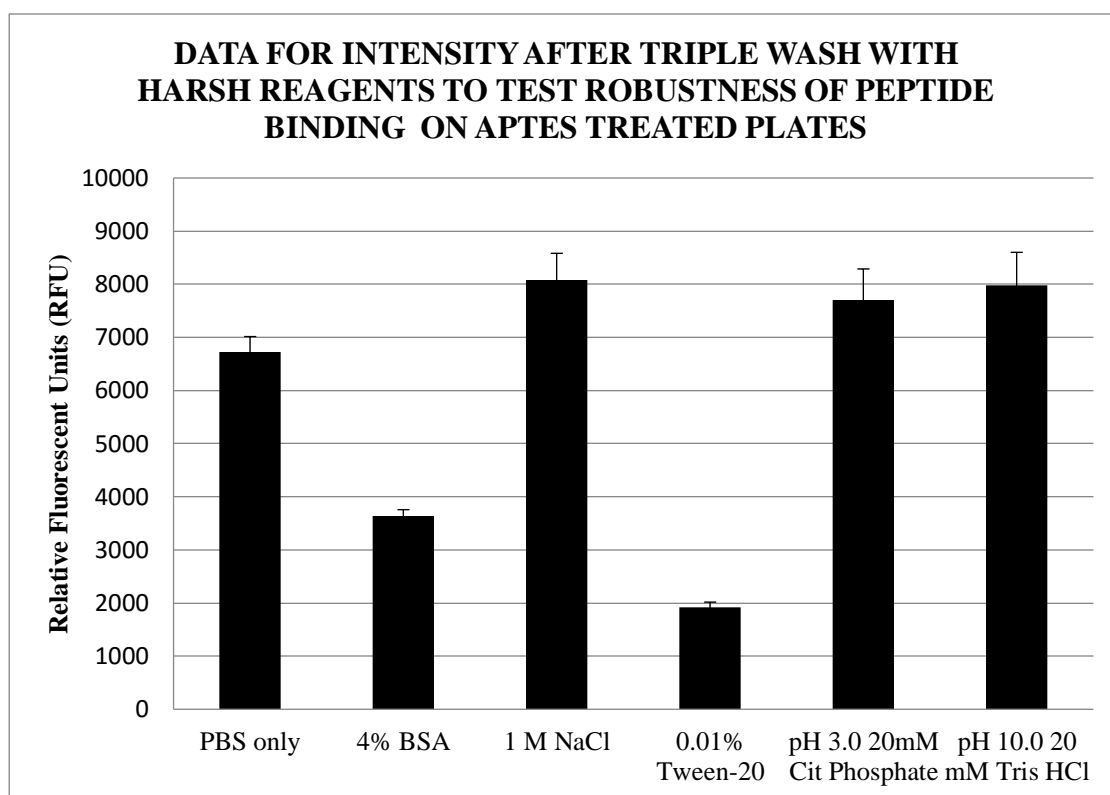


Figure 2.5: Fluorescent intensity data for 1 μM peptide labeling on APTES treated plates. The wells were washed with 100 μL of the labeled chemical on day 2 to test robustness of the attachment.

was observed that 4% BSA and 0.01% Tween-20 led to peptide dissociation, perhaps due to the peptide binding non-specifically to the plate surface. Even after the addition of a blocking step, a reduction in signal was observed upon washing with 0.01% Tween-

20 on APTES treated plates, as shown in Figure 2.6. The Covalink plates helped minimize the total number of conjugation steps; however the data generated was not reproducible or consistent, even after multiple optimization steps. Figure 2.6 also suggests that there is a small amount of increase in the fluorescent signal upon washing with 0.01% Tween 20 in the Covalink NH plates, but this change is so minute that the

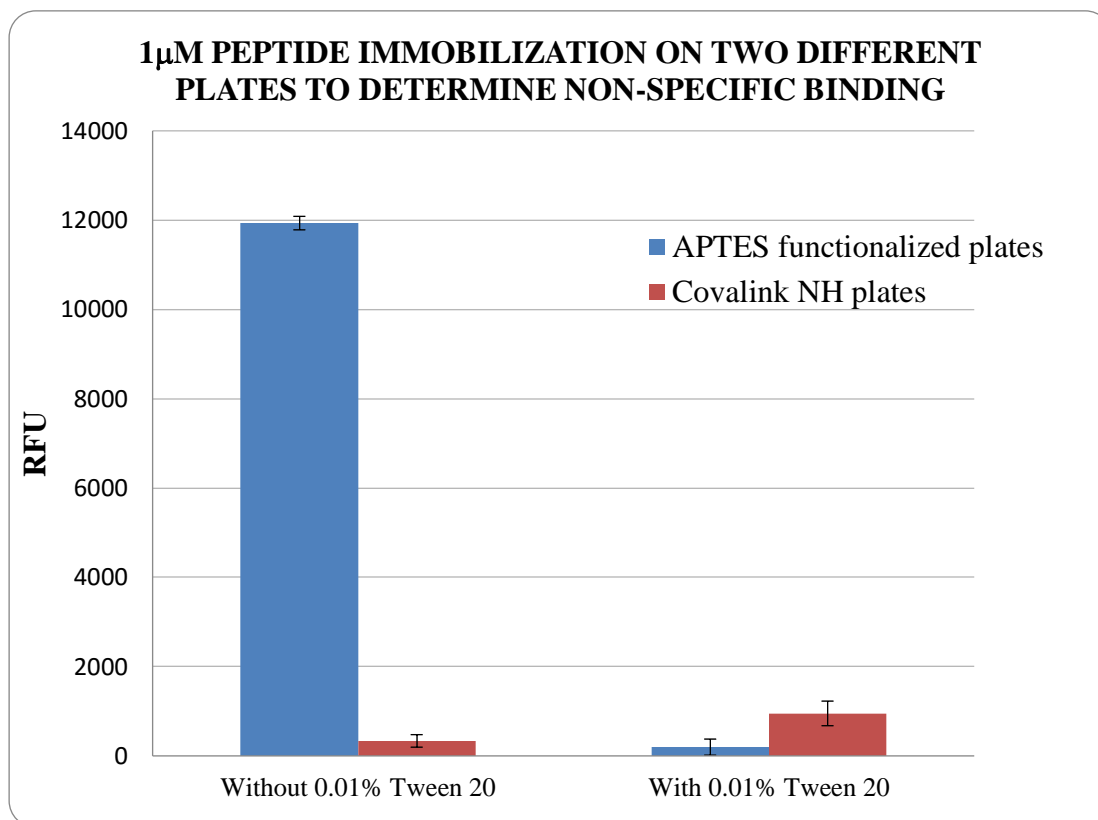


Figure 2.6: Comparison of peptide labeling between APTES treated and Covalink plates. The plates were immobilized with 1 μ M peptide and readings were taken after streptavidin conjugation.

results are inconclusive. The results indicate that the binding between the peptide and the amine functionalized plates was mostly non-covalent. Therefore, to improve the quality of the signal and consistency lacking in the EDC/NHS approach, a more robust and specific labeling chemistry was explored. The next section is going to cover the methods and materials used behind this strategy.

2.3 Immobilization Scheme 2: Cysteine-Maleimide Coupling

2.3.1 Underlying chemistry

Sulfhydryl groups have been used as targets for protein conjugation and labeling in many studies [39-42]. They are naturally present in the side chain of cysteine amino acid, therefore peptides and proteins containing cysteine residues can be coupled to a sulfhydryl reactive chemical group. One such chemical cross linker is maleic acid imide or maleimide, a derivative of the reaction between maleic anhydride and ammonia or an amine derivative [43]. The double bond of a maleimide molecule undergoes an alkylation reaction with sulfhydryl groups to form a stable thioether linkage, as shown in Figure 2.7. It is by far the most prevalent chemical group to be linked to a cysteine as the coupling scheme is highly specific and efficient [44]. Maleimides react specifically with thiols in the pH range of 6.5-7.5 [45]. It is important to stay within this range, as

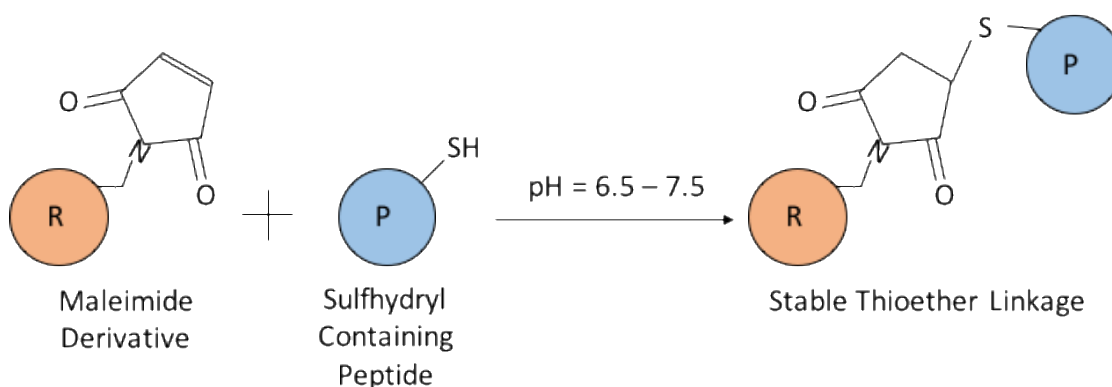


Figure 2.7: Reaction scheme from thiol coupling between maleimide and cysteine. (R) represents a reagent or crosslinker with the maleimide reactive group and (P) represents a protein carrying the free cysteine.

in more alkaline conditions ($\text{pH} > 7.5$) the reaction can be 1,000× more favorable to amines, thus leading to cross-reactivity. The cysteine-maleimide reaction is rapid and occurs in high yield to give stable thioether bonds, making it one of the most favored techniques for protein bioconjugation.

2.3.2 Materials and Methods

Black, 96-well maleimide activated plates (Pierce™ catalog number 15153) were used to perform all the initial conjugation studies. The lysine molecules on the surface of BSA are functionalized with maleimide. The this BSA is bound to the plate via passive adsorption. It was hypothesized that the free, reduced cysteine on the peptide (Fig. 2.1(b)) would react with the maleimide groups on the wells of the plate, forming a stable and irreversible bond. A binding buffer ($\text{pH} 7.2$) constituting of 0.1M sodium phosphate (Na_2HPO_4), 0.15M sodium chloride (NaCl), 10mM EDTA, and deionized water for peptide conjugation with the plate was prepared. The detailed steps for peptide attachment are illustrated in Figure 2.8. All the washing steps were performed using 100 μL of wash buffer (0.1M Na_2HPO_4 , 0.15M NaCl , 0.05% Tween-20, and deionized water, $\text{pH} 7.2$). A 0.7 mM stock of the peptide in ~11% DMSO and 89% deionized water was prepared. After initial calibration studies, it was observed that a 5 μM final concentration of the peptide gave a sufficiently high signal. For detection of signal, fluorescently labeled streptavidin with excitation/emission ~365/460 nm was used (ThermoFisher Scientific Streptavidin, Marina Blue™ conjugate catalog number S11221). The data generated from this immobilization chemistry is described in the next section. Since the eventual goal is to translate this chemistry onto the GMR sensors,

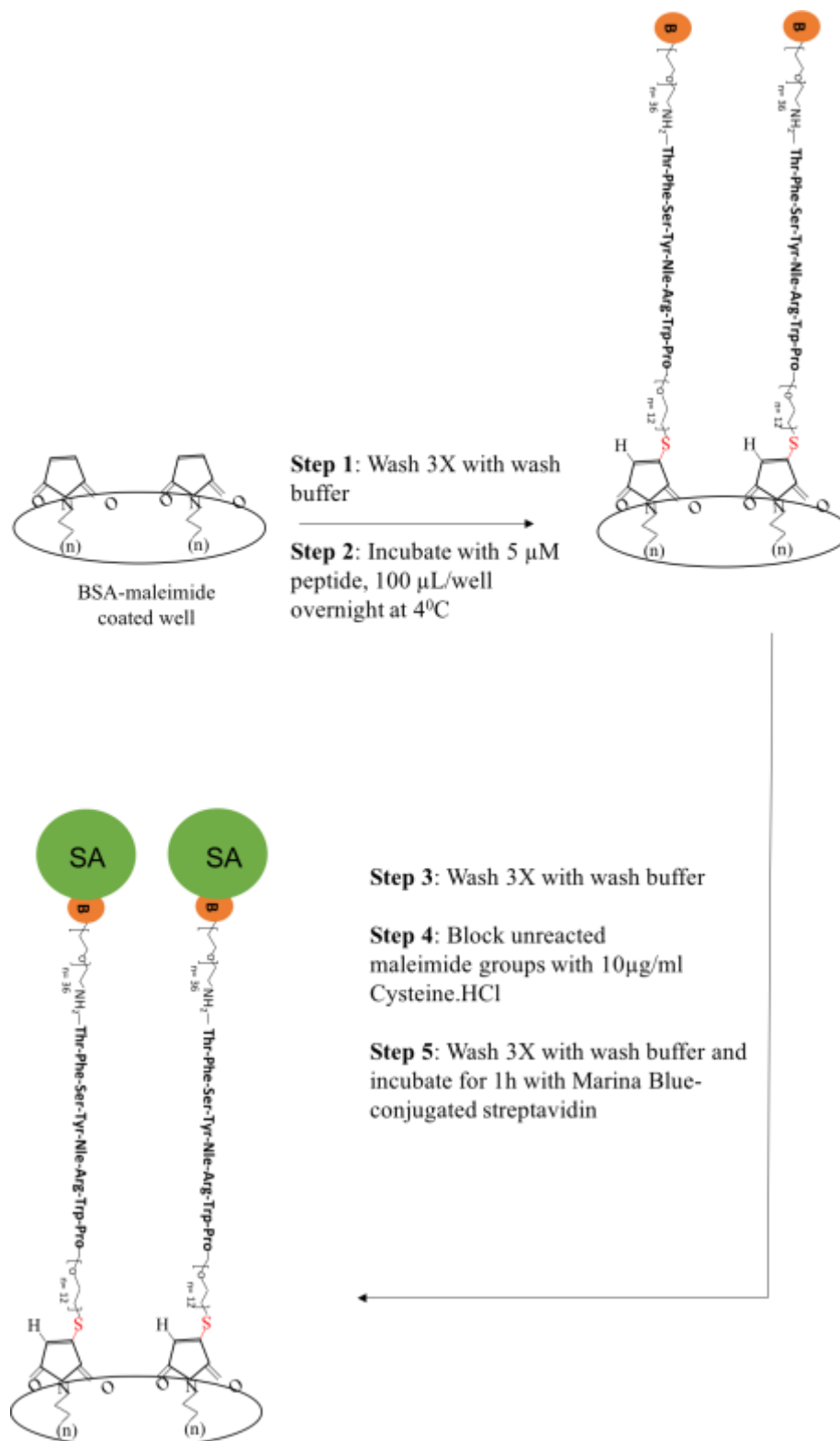


Figure 2.8: Schematic for peptide immobilization on maleimide-activated polystyrene plates.

do not come pre activated with maleimide, a similar approach was used to functionalize the plates. Instead of using the pre-activated plates, regular polystyrene plates were coated with maleimide-activated BSA [46] via passive adsorption through poly-ethyl enamine (PEI). The chemistry underlying this conjugation is illustrated in Figure 2.9. PEI is a positively charged molecule and strongly absorbs BSA at a neutral pH. A 2 mg/mL biotinylated-BSA and pure BSA (10%) were used as the positive and negative controls respectively. An assay was performed to establish an optimum concentration of BSA-maleimide by diluting it 4-fold in pure BSA, as shown in Figure 2.11.

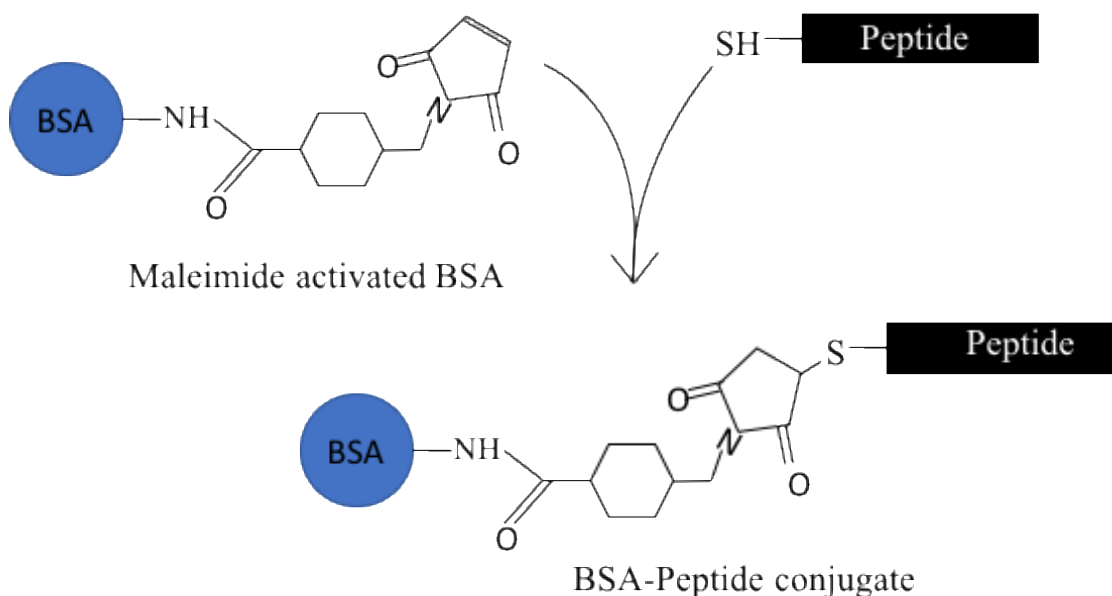


Figure 2.9: Reaction chemistry between maleimide-activated BSA and my peptide. The wells are first exposed to the maleimide-activated BSA either for 1 hour at room temperature or overnight followed by peptide conjugation for 2 hours at room temperature.

2.3.3 Results and Discussion

Unlike the EDC/NHS chemistry, this approach proved to be much more efficient and robust, as well as involving fewer and simpler steps. As shown in Figure 2.10, it was found that even after repeated washing in wash buffer (containing 0.05% Tween-20), the labeling was consistent across rows with minimal deviation from the mean

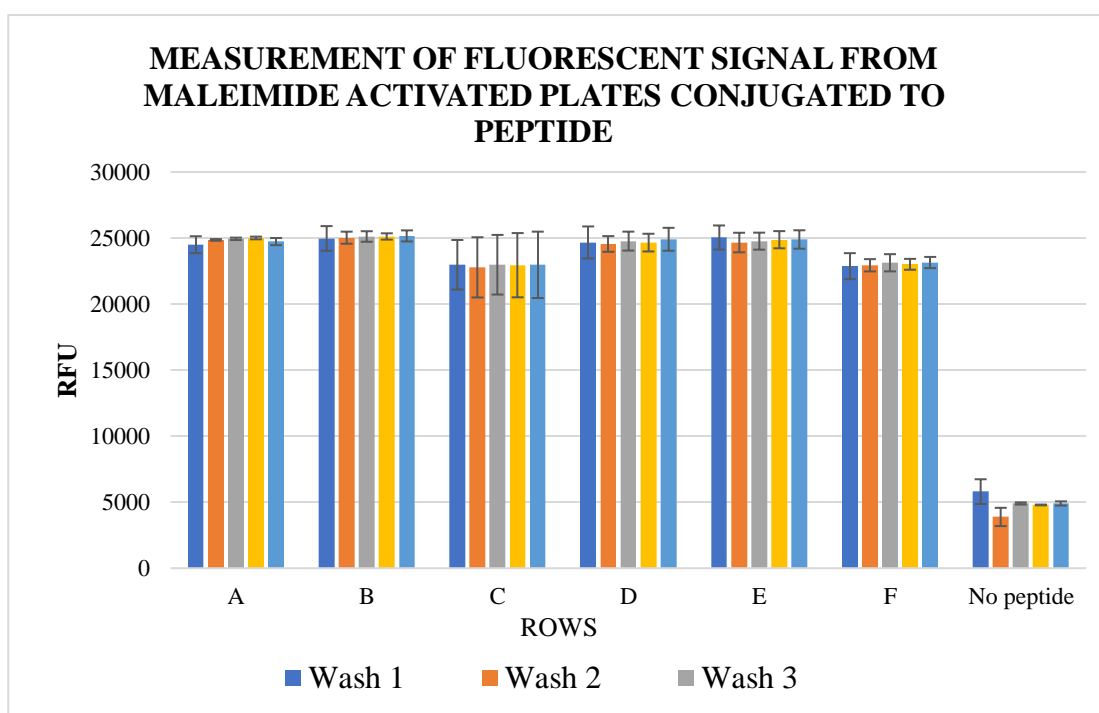


Figure 2.10: Fluorescent readings from assay to quantify peptide attachment on pre maleimide-activated plates. A 5 μM peptide concentration was used and incubated overnight at 4°C. Wash buffer described 2.3.2 was used to do the triple washes and Streptavidin-Marina Blue (MB) was used for signal detection. All readings were taken in 100 μl PBS.

fluorescent signal values. In addition, a 76% increase in signal was achieved as compared to the wells that did not contain any peptide, but followed the remaining conjugation protocol. Apart from row C, which is an anomaly, it was observed that all other rows gave a consistently high fluorescent signal, much larger than what was

achieved with the EDC/NHS approach. Next, digestion assays were performed on these plates using proteases which will be discussed in the next chapter.

With the maleimide-activated BSA approach, robust attachment was achieved a

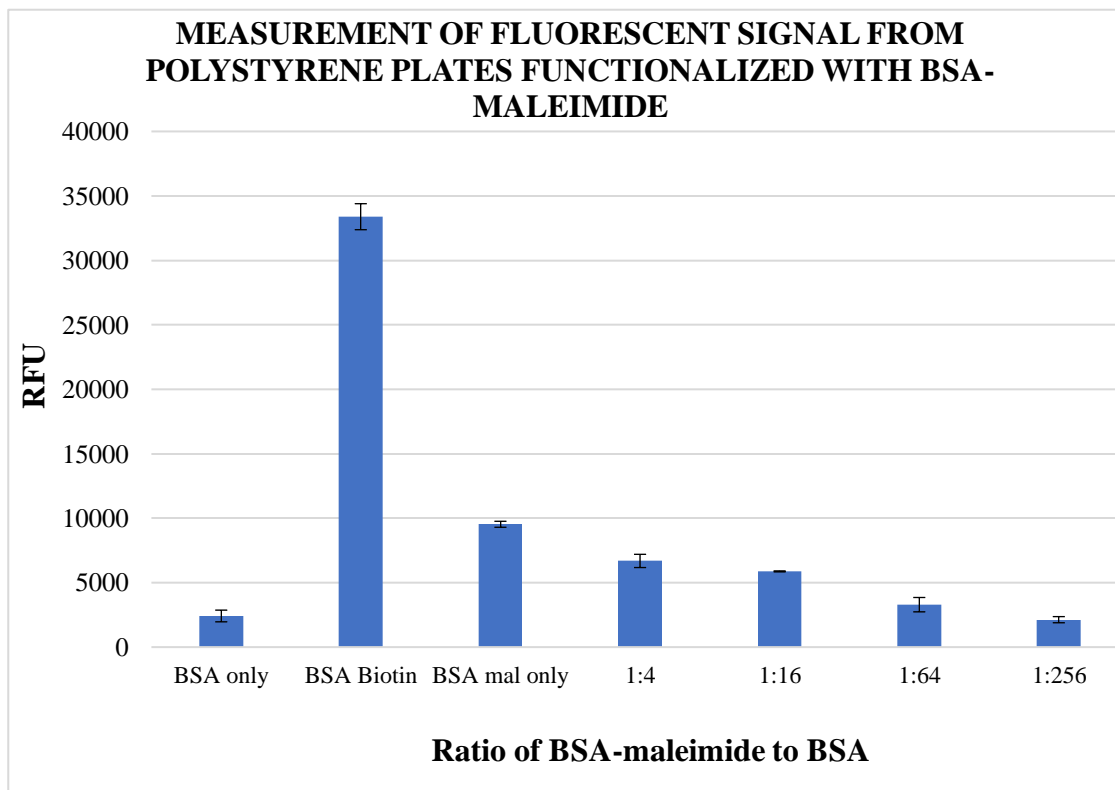


Figure 2.11: Fluorescent readings from assay to optimize concentration of BSA-maleimide required for robust attachment of the peptide. The PEI treated plates were incubated with BSA-maleimide for 1 hour at room temperature and then with peptide overnight at 4°C. The next day they were triple washed and incubated with Streptavidin MB for detection of signal.

linear decrease in fluorescent signal with reducing amount of BSA-maleimide was observed. As expected, the wells containing only 10% BSA gave a very low background signal compared to the positive control of biotinylated-BSA, which gave a very strong signal. These results indicated that the peptide was stable and robustly attached to the plate surface. The next chapter is going to highlight the protease assays performed on these plates as well on the GMR sensors.

CHAPTER 3: Protease Assays

3.1 Protease Biochemistry

Proteases are enzymes that degrade proteins by hydrolysis of a peptide bond. They are nature's "molecular scissors" and play an important role in physiological processes such as tissue remodeling and wound healing. Proteases, or sometimes often referred to as peptidases, represent the largest section of post-translational modifying enzymes in the human proteome [47] and form almost 2% of the human genome [48]. Their unregulated activity can trigger onset of many diseases like cancer, myocardial infarction, and chronic respiratory diseases. Proteases are extremely diverse in terms of their specificity with most of them being relatively non-specific for substrates, that is the same protease will target multiple peptide sequences in an "indiscriminate manner" [49]. However, some proteases are highly specific and only cleave substrates with a certain sequence. Therefore, they can be used as biomarkers for detection of specific diseases.

Many studies have been published in literature based on protease activity measurement as a tool for disease diagnosis, drug discovery, and disease staging. For example, serine protease prostatic acid phosphatase (PSAP) [50] has been shown to be an early stage biomarker for detection of ovarian cancer. Another group has developed a platform for detection of two proteases, trypsin and matrix metalloproteinase - both known to

play a role in cancer metastasis – by monitoring cleavage of a peptide sequence [51] Kaman *et al.* [52] and others have also demonstrated the use of a protease-based approach to diagnose Periodontitis. Proteases have also been characterized as virulence factors to be used in therapies for diseases such as acquired immunodeficiency syndrome (AIDS) [53]. However, most of these studies are limited by the assay sensitivity, specificity and ease of on-site detection and analysis. Fluorescent and colorimetric ELISA-based methods rely on instruments like a spectrophotometer thus rendering them difficult to implement for use in low-resource settings. Therefore, the goal of this study is to develop a rapid and simple platform for detection of protease-based infections using magnetic sensors.

3.2 Optical Digestion Assays

3.2.1 Introduction

Before testing this setup on the magnetic sensors, digestion studies were first carried out on 96 well optical plates to establish an optimized working protocol. This section will cover all the experiments performed to prove that the immobilized peptide functionalized in Chapter 2, does indeed get cleaved in the presence of a protease. The peptide sequence was first validated using an internally quenched fluorescent substrate and found that it was cleaved by Sap6 within 40 minutes of adding the enzyme. In addition, the fluorescent substrate was also cleaved by Papain, a commercial protease extracted from papaya [54], within 1 minute (Figure 3.1) adding Sap6. All following

studies were performed using papain instead of Sap6 as it is available in abundance and ideal for optimization and proof-of-concept studies. Next, digestion studies were

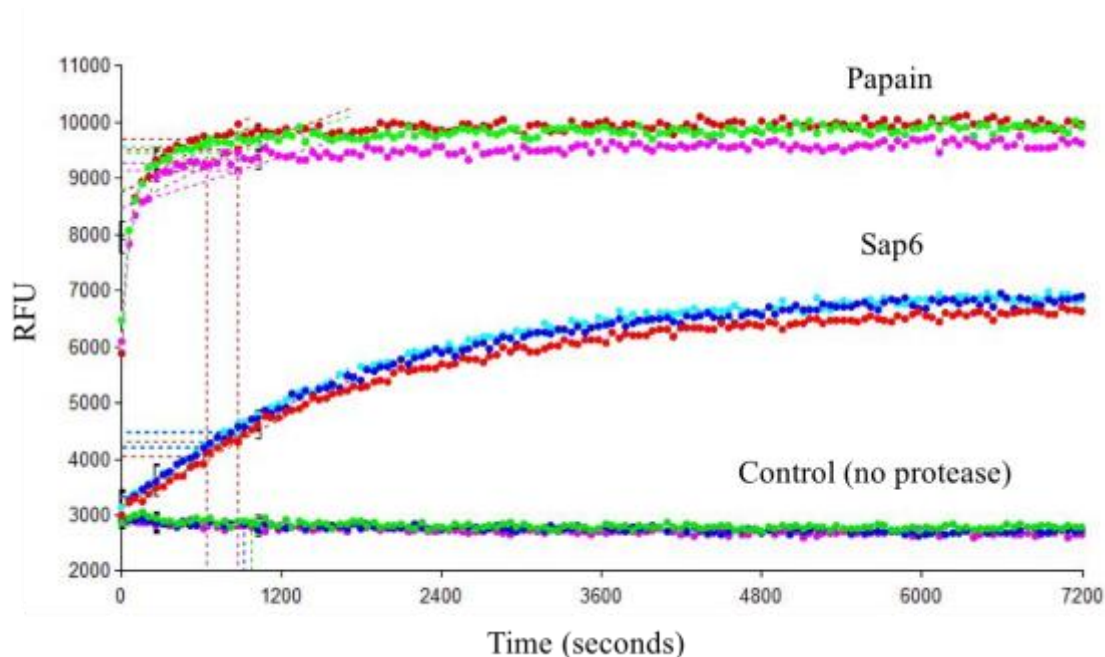


Figure 3.1: Curves representing RFU values for cleavage reaction between the fluorescently labelled peptide and Sap6 and papain. The reaction with papain is so rapid that the linear portion of the curve could be read by the plate reader. For both the proteases, the RFU values are at least $2\times$ higher than background thus indicating cleavage of the peptide sequence.

conducted on polystyrene plates to prove that an immobilized substrate is still cleavable by the protease in the same fashion as in solution. The reaction steps, conditions, and procedure are outlined in the section below.

3.2.2 Methods and Results

All the reagents used are commonly available solutions in a chemistry lab. Two approaches to perform digestion assays on the optical plates were explored. First, pre-activated maleimide labelled plates were used to optimize the protease working

conditions and prove that the immobilized substrate functionalized in section 2.3.2 gets cleaved by the protease. For this, an initial “before” read is taken to record the increase

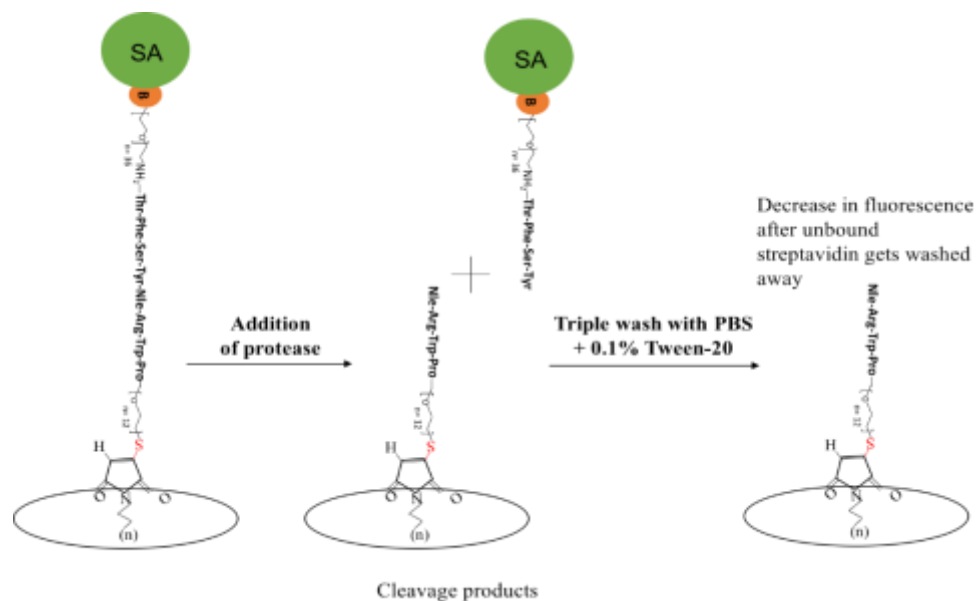


Figure 3.2: Schematic illustrating the steps involved in setting up a digestion assay after the peptide is immobilized. 100 μl of the protease, papain, is added at a concentration of 5.69 μM and incubated for 20-30 minutes at room temperature.

in signal after adding the streptavidin followed by an “after” read which is taken after the protease addition step and wash, as described in Figure 3.2. It was hypothesized that during protease incubation, several substrates will get cleaved and be released from the surface after washing with PBS and Tween-20. An experiment was conducted to obtain a time-dependent digestion curve for papain by stopping the reaction at different time intervals with a common protease inhibitor called E-64. The reaction set up is illustrated in Figure 3.3 where each row represents a unique time interval, and the columns are triplicates of the same reaction condition. 100 μl of 5.69 μM papain in buffer containing 20 mM citrate phosphate (pH 5.5), 2.7 mM KCl, 140 mM NaCl, and 0.01% Tween-20 in dH₂O was added to each row except row A, and then 11 μl of 100 μM E-64 added to

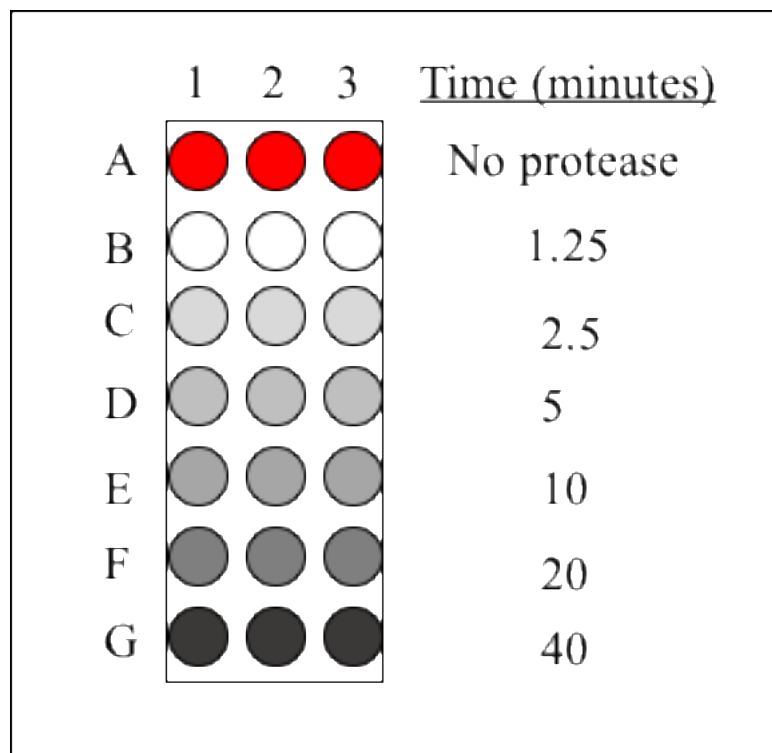


Figure 3.3: Reaction wells setup for time-dependent digestion of peptide with 5.69 μM papain. The right column indicates the time points when E-64 was added.

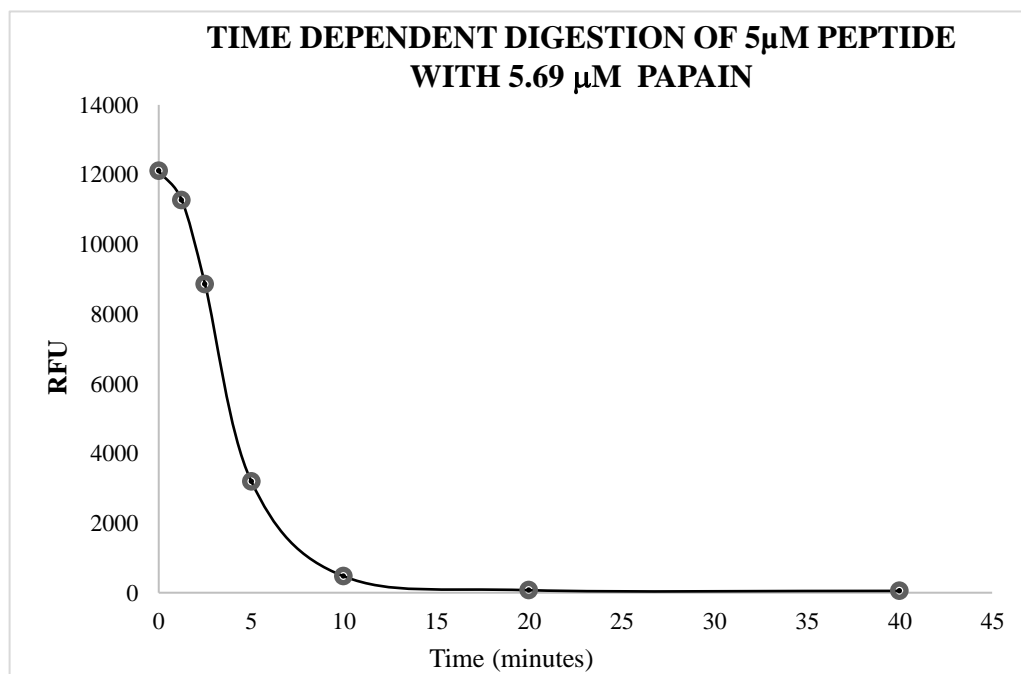


Figure 3.4: Reduction curve for time-dependent digestion of peptide with 5.69 μM papain.

well at the given time interval. The plate was incubated at room temperature throughout this step. The digestion curve is shown in Figure 3.4, where one can see that the signal drops to a negligible value in almost 20 minutes, indicating that most of the cleavage has occurred by this time. The RFU values were normalized by subtracting the background signal generated in wells with no peptide. This experiment was repeated multiple times to check for robustness and similar results were obtained.

To confirm that the reduction was obtained indeed from the cleavage of the peptide and not due to BSA degradation, an experiment as set up where the protease was added at different levels of the peptide assembly procedure. Figure 3.5 indicates this experimental setup followed by figure 3.6 which shows the plot between the

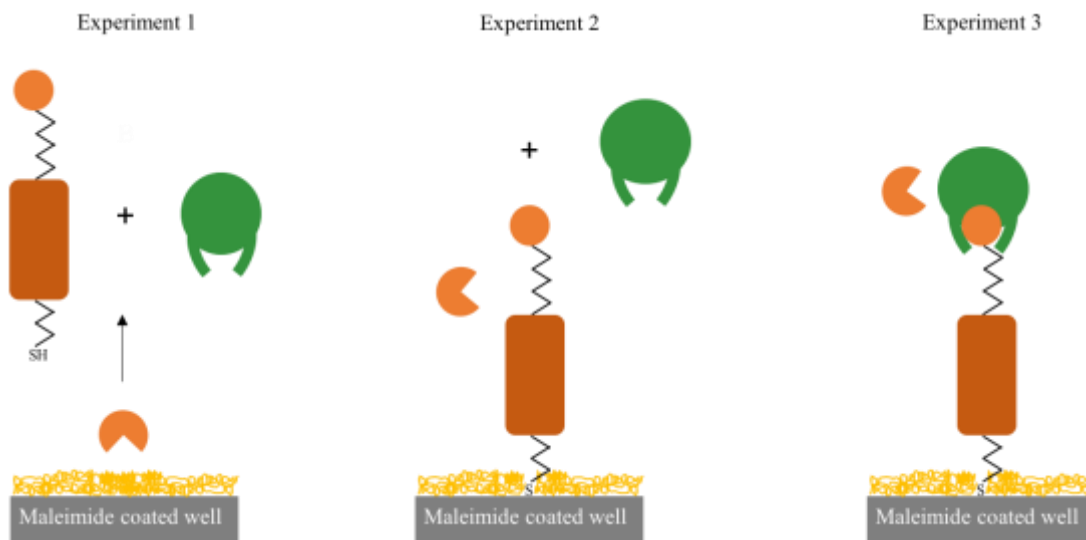


Figure 3.5: Setup of experiment to verify cleavage of peptide. In each experiment, the protease was added at different stages of the peptide assembly complex a) directly to maleimide coated well followed by peptide and streptavidin addition, b) to peptide coated well followed streptavidin addition, c) as the last step i.e after streptavidin addition. Corresponding controls were set up where no protease was added.

fluorescent readings obtained for each experiment. In experiment 1, the protease was added directly onto the maleimide coated well to test if the protease would chop up the

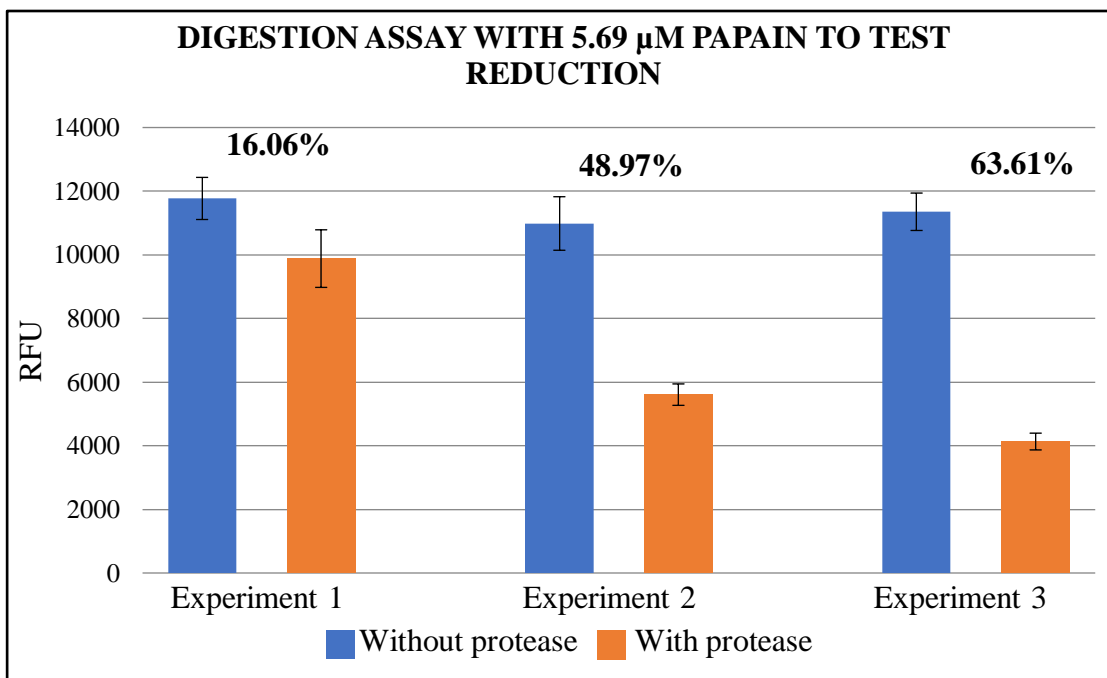


Figure 3.6: Plot of RFU values vs the level of peptide assembly at which protease was added. Before and after readings were taken in 100 μ l PBS at room temperature.

BSA or maleimides. As expected, a change in signal is observed between the wells treated with protease and the ones without, with no statistical difference, suggesting that the papain does not affect the BSA coating on the wells. Next, in experiment 2 the protease was added after peptide addition and a 50% reduction in signal was obtained, indicating that the protease was able to cleave the peptide. In the third experiment, the protease was added as the last step after streptavidin addition. In these wells also, a reduction is expected, however if the change in signal is less than in experiment 2, it would indicate that the streptavidin is causing steric hindrance to the protease. As seen from the bar plots, the reduction achieved in these wells is almost ~64%, indicating that the protease is still able to cleave the substrate. To summarize, these experiments proved two things, 1) the protease is indeed cleaving the substrate, and the reduction in signal

achieved is not due to any other factors, 2) the presence of streptavidin does not hinder the activity of the protease.

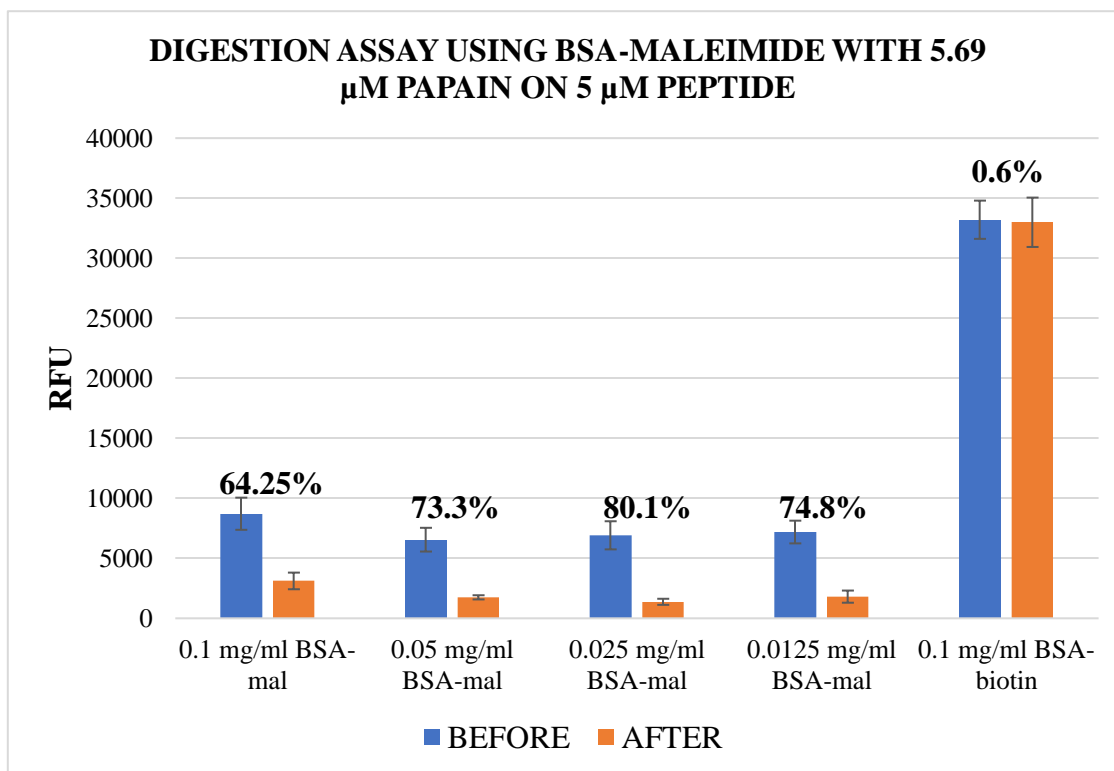


Figure 3.7: Plot of RFU values vs concentration of BSA-maleimide. The readings were taken after incubation of the protease for 20 minutes at room temperature.

Next, the second approach i.e. via manual activation of 96-well plates through BSA-maleimide was tested. This was conducted to exactly replicate the assay conditions and surface chemistry on the sensors, since the sensors are not pre-activated with maleimide groups. The assay was set up with decreasing concentrations of BSA-maleimide and incubated them overnight with peptide. In Figure 3.7, the data was normalized by subtracting the background signal from wells incubated with native BSA only. After peptide incubation and blocking with cysteine, papain was added for 20 minutes and an “after” read was taken after streptavidin addition, as shown by the

orange columns. The reduction in signal across all the dilutions was more than 64% and consistent with a standard deviation of 6.5%. On the other hand, the reduction was almost negligible for the positive control of biotinylated-BSA. These results proved that the plate functionalization and peptide immobilized via BSA-maleimide is highly sensitive to cleavage by papain and suitable to be tested on the GMR sensors.

3.3 GMR sensors

3.3.1 Introduction

The use of GMR sensors as biosensors was first demonstrated in 1998 by Baselt et al. [55] to measure the intermolecular forces that bind biological analytes like DNA and antibodies. Since then, GMR sensors have found numerous applications in detection of proteins and nucleic acids [56-60]. The main benefit of magnetic biosensing is the potential to eliminate background signal and the ease of miniaturization. With biological samples naturally lacking magnetic content, the sensitivity of these sensors is higher than other conventional sensing methods. These sensors are ideal for point-of-care testing as they are compatible with silicon complementary metal-oxide-semiconductor (CMOS) technology, allowing them to be manufactured at a commercial scale at low cost, and deployed in a one-time use format. GMR sensors, commonly used as read heads in magnetic tapes and disks, are thin-film stacks composed of alternating ferromagnetic layers and non-ferromagnetic conductive spacers. GMR sensors exhibit

magnetoresistance (MR), where a change in an external magnetic field causes a change in the electrical resistance of the material. More details about the underlying physics of these sensors can be found in [61]. Each sensor is embedded onto a chip, approximately the size of a penny (Figure 3.8).

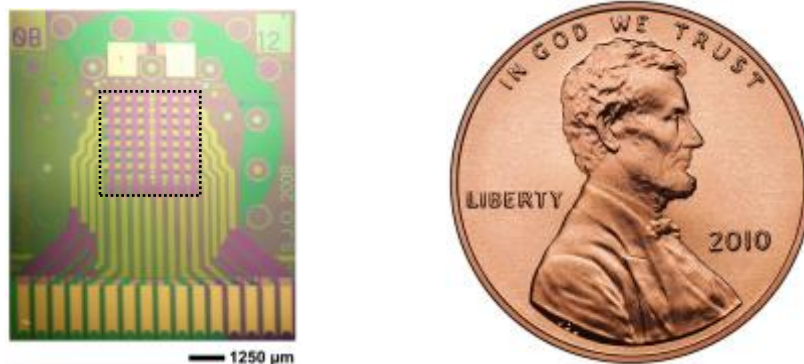


Figure 3.8: Illustration showing the GMR sensor chip. Each chip consists of an 8 by 8 array of 64 sensors indicated by the black square. The chip is 1 cm by 1.2 cm, approximately the size of a penny.

The mode of detection of signal in these sensors is via attachment of streptavidin MNPs or MACS [62-64]. These are 50 nm clusters of 10 nm Fe_2O_3 cores embedded in a dextran matrix as shown in Figure 3.9(a) [65]. The MNPs are superparamagnetic in nature and they magnetize and orient themselves in the direction of an applied external magnetic field. They generate a stray field which radiates outwards pointing from the north pole back to the south pole. This field opposes the applied local field thus causing a change in the resistance of the sensor via its free layer, as shown in Figure 3.8(b). When the applied field is removed, thermal energy causes the nanoparticles to demagnetize and randomly orient again, without bundling. The sensor is only sensitive

to nanoparticles that are within 200 nm of the surface [66], therefore any unbound nanoparticles do not need to be washed away. It is also important to note that the MNPs are colloiddally stable and they do not settle over time on the sensor surface hence

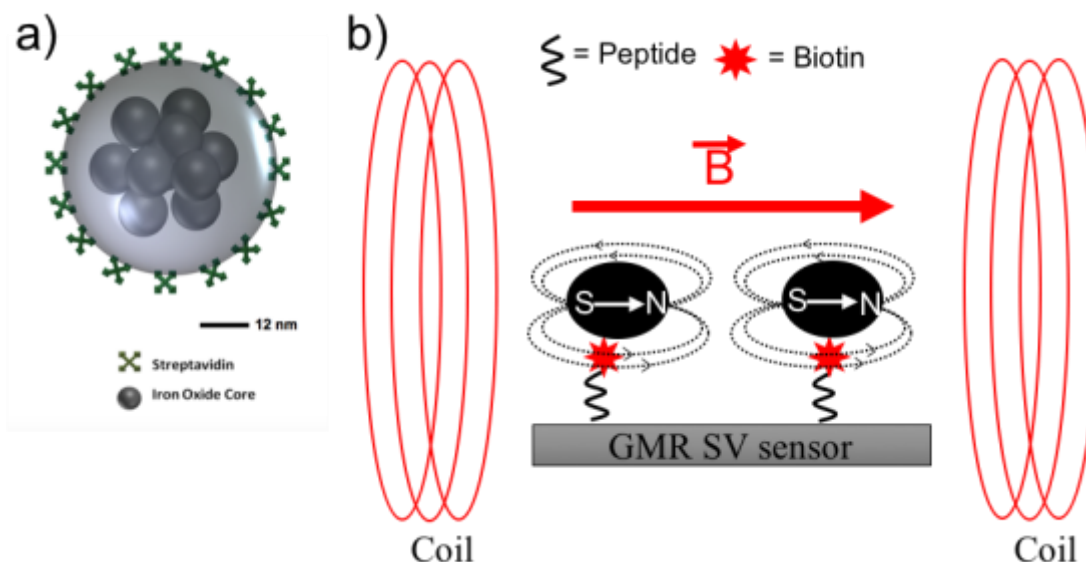


Figure 3.9: Measurement setup showing 50nm streptavidin coated superparamagnetic nanoparticles (MNPs). An external magnetic field causes the superparamagnetic MNPs to become magnetized and oriented in the same direction. The stray field from the MNPs creates a loop which opposes the external field at the sensor, and therefore reduces the field and resistance of the sensor.

reducing any nonspecific binding.

3.3.2 Chip Fabrication and Functionalization

All GMR sensors used throughout this research were purchased pre-made from MagArray Inc. The chips consist of an eight by eight array of GMR spin-valve (SV) sensors each measuring $90 \mu\text{m} \times 90 \mu\text{m}$. The sensors are coated with a thin passivation layer of SiO_2 to protect them from corrosion. A detailed description of the fabrication procedure can be found in [67]. As seen in the inset of Figure 3.10, each of the 64

sensors can be accessed by addressing a specific row and column from the 8×8 matrix. The magnetoresistance curve of a GMR sensor is shown in Figure 3.10, as described in [61]. It plots the applied external field on the x-axis versus the resistance of the sensor

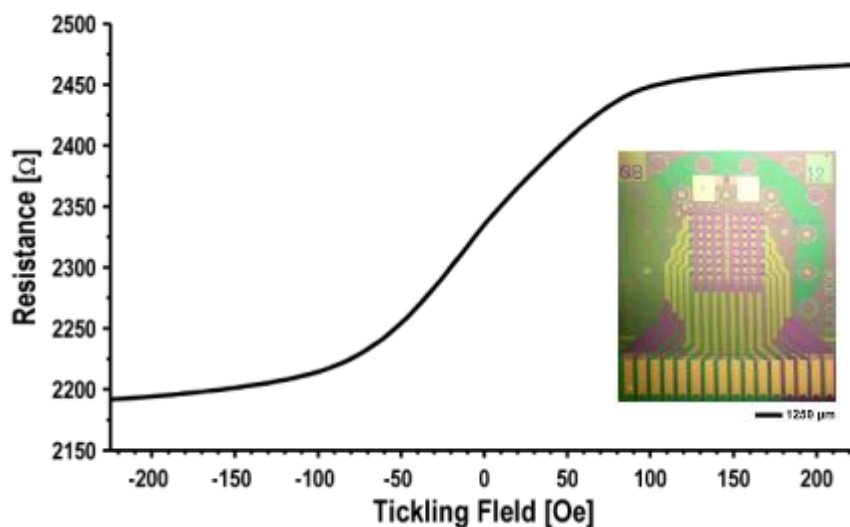


Figure 3.10: Transfer curve of a GMR SV sensor with the inset showing a photograph of the 16-pin sensor die. The chip is an 8×8 array of 64 sensors,

on the y-axis. The external field used for the experiments in this study was optimized to ~ 25 Oersted (Oe).

Prior to use, all the chips were triple washed with acetone, methanol, and isopropanol in the given order for about 30 seconds each, without allowing the chip to dry between the washes. The washing process is finished by carefully drying with nitrogen gas. Step-by-step instructions for preparing and functionalizing the chip are presented below:

1. **Reaction well fabrication** – Place a $200 \mu\text{l}$ reaction well for pipetting different reagents onto the chip using tygon tube (Figure 3.11). Cut out a ~ 7 mm well and rinse it thoroughly with Micro 90 solution. Use a two-

component epoxy to attach the well on the surface of the sensor and allow it to rest for 2 to 5 hours.

2. **Ultraviolet (UV) ozone cleaning** – Place the chip inside a UV ozone cleaner for 3 minutes to remove any organic residues on the surface.
3. **Surface functionalization** – Add 100 μl of 2% (weight by volume) polyethyleneimine (PEI) onto the sensor surface and incubate for 2 minutes. Rinse the chip 5 \times with 100 μl deionized water. Place the chip on a hot plate set to 120°C for 5 minutes to solidify the adsorbed PEI. The purpose of adding PEI is to introduce positive charges on the chip surface that will help bind the BSA via passive adsorption. Next, allow the chip to cool to room temperature and then spot with BSA and incubate for 1 hour at room temperature. When using BSA-maleimide, it is ideal to leave the chip overnight for best results. Figure 3.10 shows a sample chip spotted with BSA (negative control), BSA-biotin (positive control), and BSA-maleimide. Leave a few blank sensors between the three samples and spot about 0.2 – 0.3 μl per sample.

Since an extremely small volume of the three BSA samples is added, it is adequate to use the stock concentrations directly without diluting them down further (Table 1). After BSA incubation, a triple wash is done with a rinsing buffer (RB) consisting of 1% BSA and 0.2% Tween-20 in PBS. Next, 5 μM of the diluted peptide in binding buffer is added and the chip is incubated in a humidity chamber overnight at 4°C. The peptide would bind to the exposed maleimide groups on the surface via

reaction chemistry shown in Figure 2.7. At this point, the chip surface is completely functionalized and ready to be measured using the magnetic nanoparticles.

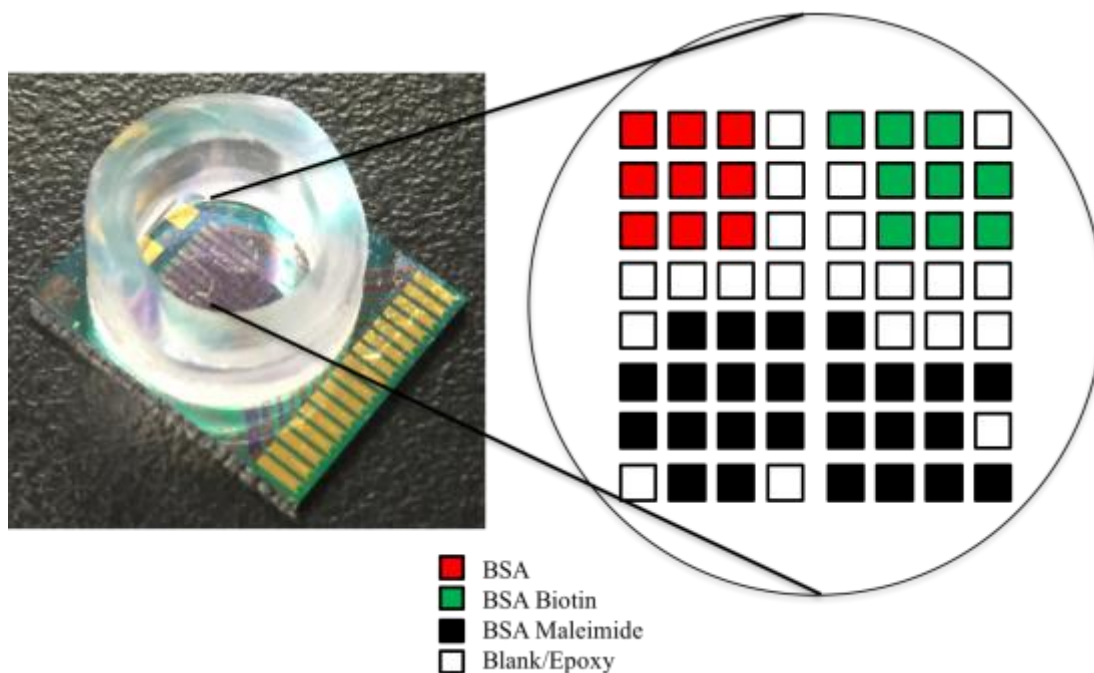


Figure 3.11: Reaction well showing the fabricated tygon tube well attached via epoxy on the chip and a sample set up of the sensor spotted with pure BSA, biotinylated BSA, and BSA-maleimide.

Table 3:1: Concentrations of the BSA samples used to functionalize the sensors.

Sample	Concentration used to spot 0.2 μ l on chip
BSA	100 mg/ml
Biotinylated BSA	2 mg/ml
Maleimide-activated BSA	10 mg/ml

3.3.3 Analysis and Measurement Setup

To measure the change in resistance of the sensors due to the presence of the magnetic nanoparticles, a custom written LabVIEW software was used, that interacts with a 64 channel biochip reader. Both the LabVIEW software and the MagDAQ64 hardware were designed by my advisor, Drew A. Hall and are described in his thesis [61]. The detection platform also consists of a power amplifier and two Helmholtz coils to generate an external magnetic field. After the chip has been functionalized with the peptide, I do a triple wash with RB and add 100 μl of PBS and transfer the chip to the

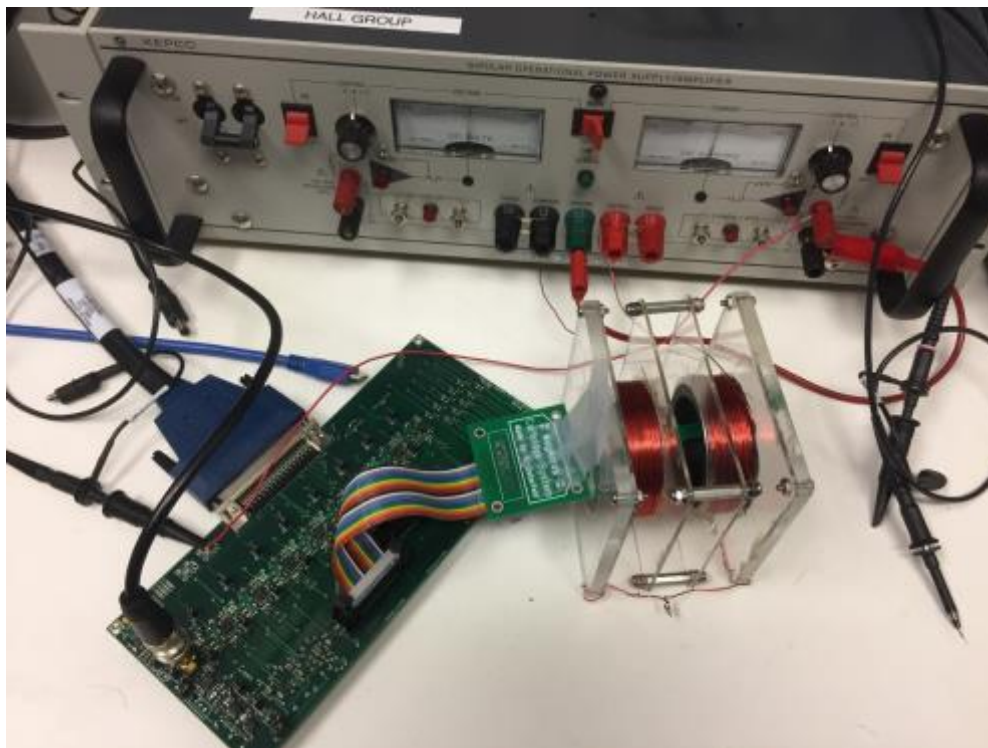


Figure 3.12: Measurement setup showing the readout circuitry, the Helmholtz coils, and the power amplifier. The chip is placed in between the coils which generate an external magnetic field.

measuring station shown in Figure 3.12, with the contact pins inserted all the way in. The LabVIEW software is designed in such a way that it lets the user enter basic information like operator name and chip ID, as well as add comments for each subsequent step, which are later exported to a .csv file. The user interface is shown in Figure 3.13, with the bottom grid corresponding to each sensor, that the user can

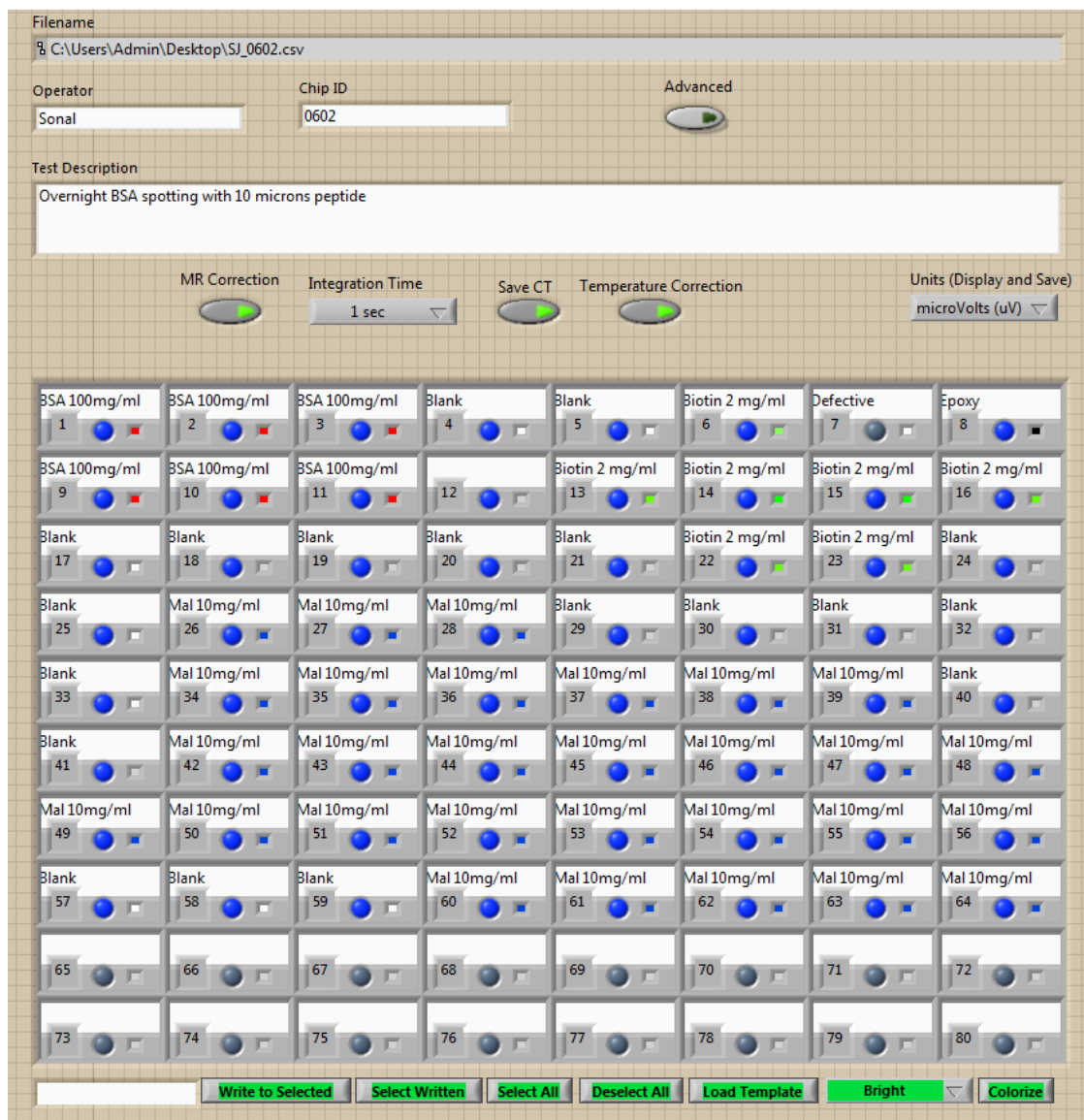


Figure 3.13: LabVIEW user interface showing the sensor grid. Each sensor has been colorized and labeled according to the surface functionalization. The bottom two rows are turned off as the chip only has 64 sensors.

colorize and label. The user should also deactivate the bottom two rows (grey) as there are only 64 sensors on this chip. Once the amplifier is turned on and the user presses START, the system goes through a series of automated steps and then displays the real-time reading to the user, every 5 seconds. One of the first experiments carried out on the GMR sensors was a control test using biotinylated-BSA. The chip was functionalized as described earlier, but this time only 100 μ l of biotinylated-BSA is added on the surface. The results are displayed in Figure 3.14. The top left grid displays the resistance of the sensors whereas the bottom left grid shows the real-time snapshot

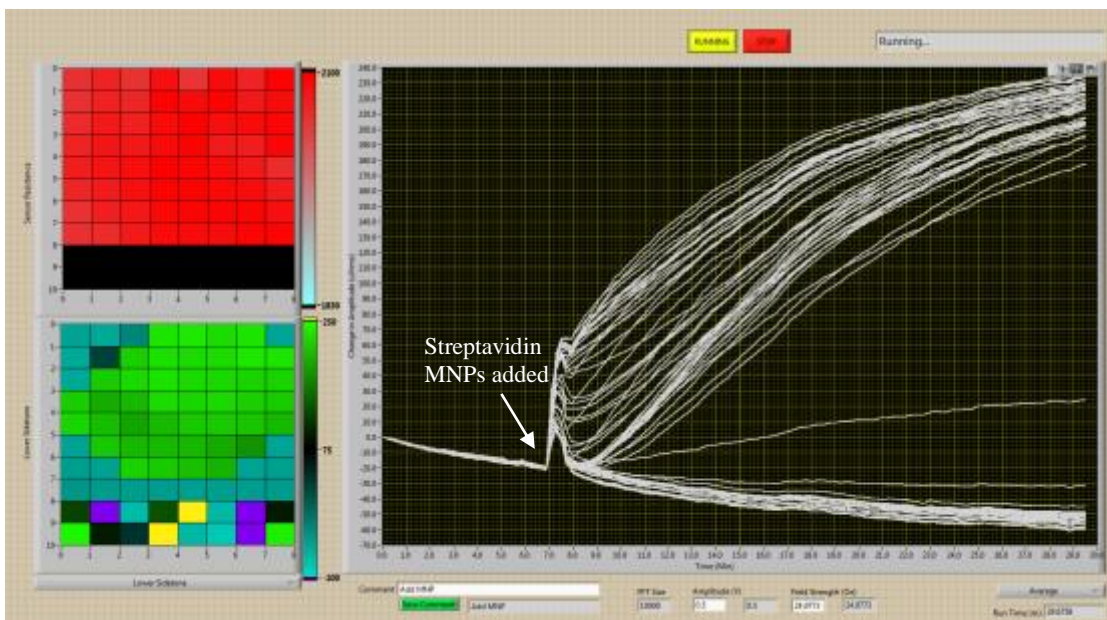


Figure 3.14: Screenshot of measurement data from pilot study ran to test BSA functionalization. Upon addition of the MNPs, we see an immediate rise in signal indicating that the streptavidin is bound to the biotin present on the chip surface.

of the sensor amplitude, where green or yellow correspond to the highest value and blue or black indicates a defective sensor. Again, it is important to note that the bottom two rows are invalid for this chip, as there are only 64 sensors. The plot on the right shows the curves for the change in magnetoresistance vs. time for each sensor in real-time. The

chip is allowed to stabilize for the first few minutes, after which the PBS is pipetted out and 40 μl of Streptavidin MNPs are added. The biotin on the chip surface binds to streptavidin and tethers the nanoparticles to the surface, increasing the change in the magnetoresistance of the sensor. This was an important result for the follow-up experiments with BSA-maleimide, as it proved that that BSA functionalized this way is stable on the chip and produces a detectable signal.

3.3.4 Results and Discussion

After verifying cleavage of the peptide on the optical plates, digestion assays on the GMR chips were tested. Several studies were carried out and subsequent changes in the procedure were made to achieve the results shown in Figure 3.15. For all the experiments performed, 4-5 sensors were functionalized with BSA, to serve as negative controls, as there should be no peptide binding to these sensors and hence no MNP signal. 6-7 sensors are also functionalized with biotinylated-BSA, to serve as my positive controls, as these would bind to the MNPs but not the peptide, and hence generate a positive signal. Lastly, 10-12 sensors were covered with BSA-maleimide to immobilize the custom peptide. Some sensors were left blank in between the three spotted samples to ensure they remain isolated from eachother (Figure 3.11).

In the initial studies performed, optimal binding kinetics of the MNPs was attained, however observed no reduction in signal ever after 2 hours of incubation with 5.69 μM peptide. The assay was improved by modulating the procedure in several ways. The main difference between the digestion assays performed on GMR sensors versus optical

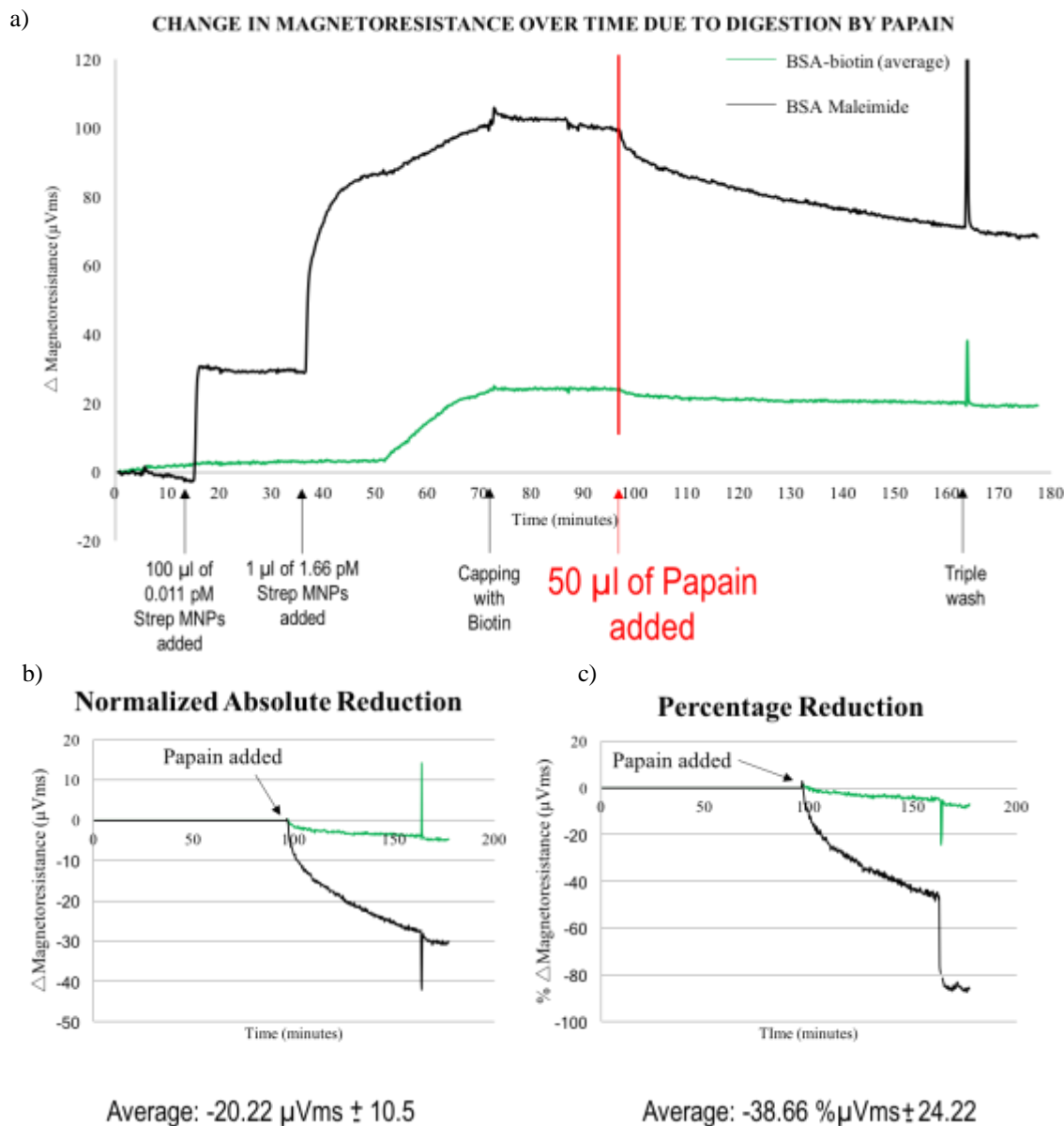


Figure 3.15: Data readout of real-time binding and release of MNPs from the sensor on chip 0802.

For the sake of simplicity, only one of the data curves is shown. This chip was incubated with BSA, BSA-biotin, and BSA-maleimide overnight at 4°C. The next day it was washed with WB and incubated with 10 μM peptide for 2 hours at room temperature. It was then blocked with cysteine for 1 hour and with buffer containing 0.1% BSA and 0.2% Tween-20 for 1 hour each. Next, it was transferred to the measuring station, where streptavidin MNPs are sequentially added and the binding kinetics are recorded for ~70 minutes. Next, 800 μM of biotin is added for 15 minutes, and as the last step 50 μM papain is added to observe the release of MNPs, a) plot of entire readout with labels for each step. The negative control sensors functionalized with BSA are subtracted from the remaining sensors, b) normalized reduction in signal obtained by subtracting the MR value of the last time point before papain addition from all subsequent data values, c) percentage reduction in signal obtained the same way as b).

plates is the mode of detection. The MNPs are much bigger in size ($\sim 10\times$) compared to the fluorophore - labelled streptavidin, therefore the steric hindrance and binding kinetics can differ between the two. Additionally, the MNPs are conjugated to multiple streptavidin molecules, which can cause them to bind to multiple peptide molecules at once, increasing the cleavage time and kinetics. It was also hypothesized, that after being released by the protease, the MNPs, via their free streptavidins, are binding to other biotinylated-peptides on the surface that remain unbound. To mitigate this, an additional blocking step after MNP addition was performed, by adding pure-biotin to the reaction well. This would cap the remaining streptavidin molecules on the MNPs that are not bound to the peptides.

Next, the pH of the protease buffer was changed from the initial 5.5 to a neutral 7.2, where all the other assembly steps are being carried out, to reduce the number of variables affecting the peptide structure. The protease concentration is also dialed up to a maximum of 50 μM , after initial studies that did not result in any cleavage at the regular 5.69 μM concentration of protease being used on the optical plates. The last optimization step carried out was to increase the BSA incubation step, from one hour at room temperature to overnight at 4°C. This change considerably improved the binding kinetics of the MNPs, perhaps due to better immobilization of the peptide. It also led to an increase in the percentage of reduction by the protease upto an average of $\sim 40\%$, as shown in Figure 3.15(c). Though encouraging, the reduction was not able to reduce to the background signal. It was hypothesized, that perhaps the streptavidin MNPs were forming a densely-packed monolayer bound to the peptide, thus preventing the protease from accessing the peptide and cleaving it. To test this, another experiment was set up

in the same way as the previous digestion assay, however this time bigger MNPs were used. By increasing the size to 1 μm , it was hypothesized that there would be more room between the packed MNPs for the protease to enter and cleave the peptide. The results from this experiment are plotted in Figure 3.16 below. Instead of plotting the real-time curves, the absolute values at specific time points were plotted as bar columns. The background signal before adding the MNPs were subtracted from each data point. The x-axis of the plot shows the functionalization and sensor number for the peptide sensors. The orange columns represent the loading value of the MNPs i.e. the time point after which there was no more binding observed. The blue columns represent the release value of the MNPs i.e. the time point after which the protease and any cleaved substrates were washed away. The negative control – blank - showed no increase in signal after addition of the MNPs, and the positive control – biotinylated BSA – gave a high signal upon loading and no reduction upon addition of the protease, as expected. For all the peptide sensors, the release signal after washing the digested peptide was reduced to

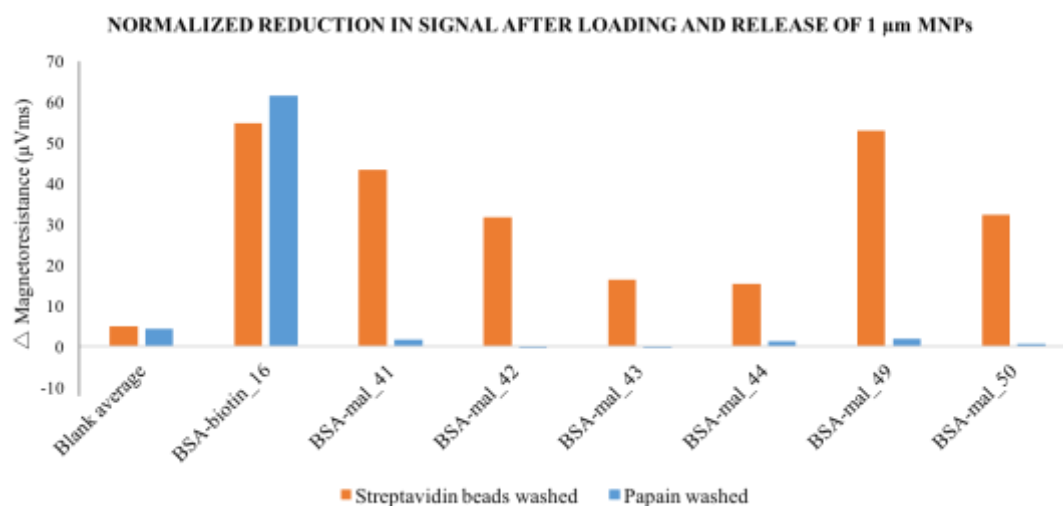


Figure 3.16: Bar plots comparing the loading and release of 1 μm MNPs after digestion with papain. The BSA-_mal sensors correspond to the peptide activated sensors. The peptide sensors reduce to background after addition of protease and washing the cleaved peptides.

background – which proved to us that the peptide was being readily cleaved by papain. These results were highly encouraging as they showed complete release of the peptide substrate after adding in the protease. However, this assay is not ideal, because the 1 μm MNPs are not colloidally stable like the 50 nm particles and need to be washed away. The overall aim of this project is to develop a wash-free assay, therefore further optimization needs to be carried out with the 50 nm particles to reduce their packing density. The results achieved on the magnetic sensors, combined with the optical assays on 96-well plates proved to us that the release of MNPs from the surface of the sensor, upon cleavage of the peptide by papain, can be monitored in real-time. There are several other factors and conditions that need to be tested further, and are discussed in the next chapter as future work.

CHAPTER 4: Conclusion

4.1 Summary

The overall goal of this research is to develop a magnetic biosensor immobilized with a pre-assembled peptide complex, which is then rapidly disassembled by a specific protease. This thesis describes the design process of this sensor platform that can detect a protease in a sample via rapid cleavage of a custom peptide sequence. 96 well assay plates were used to characterize the surface functionalization and to carry out extensive optimization studies for showing proof-of-concept. The assays were then translated to the GMR sensors where a reduction in signal was observed in less than 60 minutes. In this chapter, the key results of this work and areas of future work will be discussed.

Chapter 1 introduced the readers to biosensing platforms and provided background knowledge of the disease, Candidemia. The motivation for this work and the overall objectives were also discussed. Chapter 2 thoroughly described the strategies used to immobilize the peptide sequence onto the surface of 96 well plates, and the procedure for doing so. The key results obtained from various studies performed were also presented. Chapter 3 first described the digestion assays performed on the optical setup, later followed by my work with the GMR sensors. A summary of the working and characterization of GMR sensors was discussed, most of which was

derived from my advisor's thesis [62]. Lastly, the results achieved by carrying out protease studies on the sensors were presented. By showing significant reduction in less than 60 minutes, it was proved that a sensor immobilized with a specific peptide, via thiol coupling, can be used to detect presence of a protease in each sample.

By utilizing ELISA based detection assays on 96 well microplates, the proof-of-concept was established before transitioning to the nanosensors. A peptide with a free cysteine end was immobilize onto plates that were functionalized with maleimide. This coupling chemistry proved much more robust and efficient than the earlier proposed EDC/NHS chemistry. Within 10 minutes of adding the protease, papain, onto the peptide assembly, almost a 100% reduction in signal was achieved. This was an extremely important result, as it proved that the designed peptide sequence was susceptible to cleavage by papain and could be further tested on the portable GMR sensors.

Studies involving GMR sensors and their use as platforms for antibody recognition have mostly focused on detecting the “on” rate or the binding kinetics of the MNPs. By utilizing the unique property of proteases to cleave at a specific location on a peptide, this is the first time that the “off” rate or the release kinetics of these nanoparticles have been characterized. The reduction in magnetoresistance as the nanoparticles float away from the sensor surface, has been detected, in real-time. Since every protease molecule can cleave thousands of substrate molecules, a highly-amplified signal is generated making this detection scheme highly sensitive. This novel technology alleviates the need to perform washing steps required in a traditional ELISA

which when coupled with the enhanced sensitivity makes it an ideal candidate for point-of-care applications.

4.2 Future Directions

The focus for the future work for this study lies in further optimizing the digestion assays on GMR sensors. Currently, the system can achieve about 60% reduction in signal in 60 minutes. However, both these parameters need further improvement to increase the signal quality and lower detection time. Additionally, the digestion on GMR sensors is currently being performed at a neutral pH to reduce the number of overall variables. However, to eliminate background protease activity in blood, pH will be lowered to 5.5, where *Candida* proteases have optimal activity, but other blood proteases do not.

Currently, the peptide sequence is only being hydrolyzed by papain, which is a cysteine protease, in both the optical as well as the nanosensor setups. However, since the peptide was originally designed for cleavage by Sap6, it is perhaps some sort of an accessibility issue that is preventing the protease to go near the peptide. This can be alleviated by testing PEG- linker sequences of various lengths to find ideal conditions that allow for maximum accessibility of the recombinant Sap6 protease. The density of the peptides can also be modulated by considering mixtures of PEG-linkers. To establish a lower limit of detection, Sap6 will be serially diluted until no signal is detected. Additionally, to determine if human proteases cleave the SAP6 peptide sequence, more complex fluids like such as serum and plasma will be tested, as the experiments right now are being carried out in a stable buffer. If cleavage occurs,

protease inhibitors can be added to target serine, cysteine, and metallo-proteases, but not Sap6. Non-specific interactions of blood proteins with the peptide or surface chemistry will also be quantified.

Overall, this was a proof-of-concept of a novel method to assess the presence of a protease in each sample, via deconstruction of a peptide assembly. The eventual goal of this technology is to extend the concept to several blood borne infections, such as septicemia, toxoplasmosis, and Chagas disease.

References

- [1] Frieder W. Scheller (16)(17), Aysu Yarman (16)(17), Till Bachmann (18), Thomas Hirsch (19), Stefan Kubick (16), Reinhard Renneberg (20), Soeren Schumacher (16), Ulla Wollenberger (17), Carsten Teller (16), and Frank F. Bier (16)(17). "Future of Biosensors: A Personal View." Springer. Springer Berlin Heidelberg, 01 Jan. 1970.
- [2] Sanjay, Sharma T., Guanglei Fu, Maowei Dou, Feng Xu, Rutao Liu, Hao Qi, and XiuJun Li. "Biomarker Detection for Disease Diagnosis Using Cost-effective Microfluidic Platforms." *The Analyst*. U.S. National Library of Medicine, 07 Nov. 2015.
- [3] -John, Andrew St, and Christopher P. Price. "Existing and Emerging Technologies for Point-of-Care Testing." *The Clinical Biochemist Reviews*. The Australian Association of Clinical Biochemists, Aug. 2014.
- [4] Rajendran, Rajesh, and Gerry Rayman. "Point-of-Care Blood Glucose Testing for Diabetes Care in Hospitalized Patients: An Evidence-Based Review." *Journal of Diabetes Science and Technology*. SAGE Publications, Nov. 2014.
- [5] "What Is Mobile Health Technology | Knowledge Hub | Athenahealth." Athena Health. N.p., n.d.
- [6] And, M. A. Pfaller^{13*}. "M. A. Pfaller." *Clinical Microbiology Reviews*. N.p., 01 Jan. 2007.
- [7] – Wintera, Michael B., Eugenia C. Salcedob, Matthew B. Lohsecd, Nairi Hartoonie, Megha Gulatif, Hiram Sanchezgh, Julie Takagic, Bernhard Hubei, David R. Andesgh, Alexander D. Johnsonc, and Charles S. Craika. "Michael B. Winter." *MBio*. N.p., 13 Sept. 2016.
- [8] Leinberger DM, Schumacher U, Autenrieth IB, "Development of a DNA microarray for detection and identification of fungal pathogens involved in invasive mycoses." *J Clin Microbiol*. 2005;43:4943–4953.
- [9] Cai D, Xiao M, Xu P. An integrated microfluidic device utilizing dielectrophoresis and multiplex array PCR for point-of-care detection of pathogens. *Lab Chip*. 2014;14:3917–3924.
- [10]- Boles DJ, Benton JL, Siew GJ. Droplet-based pyrosequencing using digital microfluidics. *Anal Chem*. 2011;83:8439–8447

- [11] Schell WA, Benton JL, Smith PB. Evaluation of a digital microfluidic real-time PCR platform to detect DNA of *Candida albicans* in blood. *Eur J Microbiol Infect Dis*. 2012;31:2237–2245.
- [12] "Electrochemical Glucose Biosensors." ACS Publications. N.p., n.d.
- [13] A Review of Enzymatic Uric Acid Biosensors Based on Amperometric Detection. N.p., n.d.
- [14] Carreiro, Stephanie, David Smelson, Megan Ranney, Keith J. Horvath, R. W. Picard, Edwin D. Boudreaux, Rashelle Hayes, and Edward W. Boyer. "Real-Time Mobile Detection of Drug Use with Wearable Biosensors: A Pilot Study." *Journal of Medical Toxicology*. Springer US, Mar. 2015.
- [15] Katz, Evgeny, Vladimir Privman, and Joseph Wang. "Towards Biosensing Strategies Based on Biochemical Logic Systems." 2010 Fourth International Conference on Quantum, Nano and Micro Technologies (2010): n. pag.
- [16] Campàs, M., B. Prieto-Simón, and J. L. Marty. "A Review of the Use of Genetically Engineered Enzymes in Electrochemical Biosensors." *Seminars in Cell & Developmental Biology*. U.S. National Library of Medicine, Feb. 2009.
- [17] D. R. Baselt, G. U. Lee, M. Natesan, S. W. Metzger, P. E. Sheehan, and R. J. Colton, "A biosensor based on magnetoresistance technology," *Biosensors and Bioelectronics*, vol. 13, no. 7-8, pp. 731-739, Oct. 1998.
- [18] B. M. de Boer, J. A. H. M. Kahlman, T. P. G. H. Jansen, H. Duric, and J. Veen, "An integrated and sensitive detection platform for magneto-resistive biosensors," *Biosensors and Bioelectronics*, vol. 22, no. 9-10, pp. 2366-2370, Apr. 2007.
- [19] S. P. Mulvaney, K. M. Myers, P. E. Sheehan, and L. J. Whitman, "Attomolar protein detection in complex sample matrices with semi-homogeneous fluidic force discrimination assays," *Biosensors and Bioelectronics*, vol. 24, no. 5, pp. 1109-1115, Jan. 2009.
- [20] L. Xu, H. Yu, M. S. Akhras, S.-J. Han, S. Osterfeld, R. L. White, N. Pourmand, and S. X. Wang, "Giant magnetoresistive biochip for DNA detection and HPV genotyping," *Biosensors and Bioelectronics*, vol. 24, no. 1, pp. 99-103, Sep. 2008.
- [21] M. Koets, T. van der Wijk, J. T. W. M. van Eemeren, A. van Amerongen, and M. W. J. Prins, "Rapid DNA multi-analyte immunoassay on a magneto-resistance biosensor," *Biosensors and Bioelectronics*, vol. 24, no. 7, pp. 1893-1898, Mar. 2009.

- [22] S. J. Osterfeld, H. Yu, R. S. Gaster, S. Caramuta, L. Xu, S.-J. Han, D. A. Hall, R. J. Wilson, S. Sun, R. L. White, R. W. Davis, N. Pourmand, and S. X. Wang, "Multiplex protein assays based on real-time magnetic nanotag sensing," *Proceedings of the National Academy of Sciences*, vol. 105, no. 52, pp. 20637- 20640, Dec. 2008.
- [23] G. Li, V. Joshi, R. L. White, S. X. Wang, J. T. Kemp, C. Webb, R. W. Davis, and S. Sun, "Detection of single micron-sized magnetic bead and magnetic nanoparticles using spin valve sensors for biological applications," *J. Appl. Phys.*, vol. 93, no. 10, p. 7557, May 2003.
- [24] J. Schotter, P. B. Kamp, A. Becker, A. Pühler, G. Reiss, and H. Brückl, "Comparison of a prototype magnetoresistive biosensor to standard fluorescent DNA detection," *Biosensors and Bioelectronics*, vol. 19, no. 10, pp. 1149-1156, May 2004.
- [25] D. L. Graham, H. A. Ferreira, and P. P. Freitas, "Magnetoresistive-based biosensors and biochips," *Trends in Biotechnology*, vol. 22, no. 9, pp. 455-462, Sep. 2004.
- [26] Xu, Liang, Heng Yu, Shu-Jen Han, Sebastian Osterfeld, Robert L. White, Nader Pourmand, and Shan X. Wang. "Giant Magnetoresistive Sensors for DNA Microarray." *IEEE Transactions on Magnetics*. U.S. National Library of Medicine, 01 Nov. 2008.
- [27] nanoLAB: An ultraportable, hand-held diagnostic laboratory for global health," *Lab on a Chip*, 11, 950-956, 2011.
- [28] R. Curry, H. Heitzman, D. Riege, R. Sweet, and M. Simonsen, "A systems approach to fluorescent immunoassay: general principles and representative applications," *Clin Chem*, vol. 25, no. 9, pp. 1591-1595, Sep. 1979.
- [29] M. Han, X. Gao, J. Z. Su, and S. Nie, "Quantum-dot-tagged microbeads for multiplexed optical coding of biomolecules," *Nat Biotech*, vol. 19, no. 7, pp. 631- 635, Jul. 2001.
- [30] Syahir, A., K. Usui, K. Y. Tomizaki, K. Kajikawa, and H. Mihara. "Label and Label-Free Detection Techniques for Protein Microarrays." *Microarrays* (Basel, Switzerland). U.S. National Library of Medicine, 24 Apr. 2015.
- [31] R. S. Gaster, D. A. Hall, C. H. Nielsen, S. J. Osterfeld, H. Yu, K. E. Mach, R. J. Wilson, B. Murmann, J. C. Liao, S. S. Gambhir, and S. X. Wang, "Matrixinsensitive protein assays push the limits of biosensors in medicine," *Nat Med*, vol. 15, no. 11, pp. 1327-1332, Nov. 2009
- [32] "Profiling of Rat Plasma by Surface-enhanced Laser Desorption/ionization Time-of-flight Mass Spectrometry, a Novel Tool for Biomarker Discovery in Nutrition

Research." Profiling of Rat Plasma by Surface-enhanced Laser Desorption/ionization Time-of-flight Mass Spectrometry, a Novel Tool for Biomarker Discovery in Nutrition Research - ScienceDirect. N.p., n.d.

[33] Luo, Yiqi, Fang Yu, and Richard N. Zare. "Microfluidic Device for Immunoassays Based on Surface Plasmon Resonance Imaging." *Lab on a Chip*. The Royal Society of Chemistry, 28 Mar. 2008.

[34] G. Wu, R. H. Datar, K. M. Hansen, T. Thundat, R. J. Cote, and A. Majumdar, "Bioassay of prostate-specific antigen (PSA) using microcantilevers," *Nat Biotech*, vol. 19, no. 9, pp. 856-860, Sep. 2001

[35] Wintera, Michael B., Eugenia C. Salcedob, Matthew B. Lohsecd, Nairi Hartoonie, Megha Gulatif, Hiram Sanchezgh, Julie Takagic, Bernhard Hubei, David R. Andesgh, Alexander D. Johnsonc, and Charles S. Craika. "Michael B. Winter." *MBio*. N.p., 13 Sept. 2016.

[36] "A Simple, Rapid and Inexpensive Technique to Bind Small Peptides to Polystyrene Surfaces for Immunoenzymatic Assays." *A Simple, Rapid and Inexpensive Technique to Bind Small Peptides to Polystyrene Surfaces for Immunoenzymatic Assays - ScienceDirect*. N.p., n.d.

[37] "Carbodiimide Crosslinker Chemistry." Thermo Fisher Scientific. N.p., n.d.

[38] Corresponding Author: Sr. Technical Adviser Thomas Andersen, Thermo Fisher Scientific, Roskilde, Denmark. Coupling of Peptides to Nunc CovaLink Surfaces via Their Carboxylic Groups (n.d.): n. pag.

[39] Duncan, R. Julian S., Peter D. Weston, and Roger Wrigglesworth. "A new reagent which may be used to introduce sulfhydryl groups into proteins, and its use in the preparation of conjugates for immunoassay." *Analytical biochemistry* 132.1 (1983): 68-73.

[40] Carlsson, Jan, Hakan Drevin, and Rolf Axen. "Protein thiolation and reversible protein-protein conjugation. N-Succinimidyl 3-(2-pyridyldithio) propionate, a new heterobifunctional reagent." *Biochemical Journal* 173.3 (1978): 723-737.

[41] Brinkley, Michael. "A brief survey of methods for preparing protein conjugates with dyes, haptens and crosslinking reagents." *Bioconjugate chemistry* 3.1 (1992): 2-13.

[42] Wong, Shan S. *Chemistry of protein conjugation and cross-linking*. CRC press, 1991.

[43] Kim, Younggyu.. "Efficient site-specific labeling of proteins via cysteines." *Bioconjugate chemistry* 19.3 (2008): 786-791.

[44] Kim, Younggyu, Sam O. Ho, Natalie R. Gassman, You Korlann, Elizabeth V. Landorf, Frank R. Collart, and Shimon Weiss. "Efficient Site-Specific Labeling of Proteins via Cysteines." *Bioconjugate Chemistry*. U.S. National Library of Medicine, Mar. 2008.

[45] "Sulphydryl-Reactive Crosslinker Chemistry." *Sulphydryl-Reactive Crosslinker Chemistry* | Thermo Fisher Scientific. N.p., n.d. Web. 12 June 2017.

[46] Instructions. *Inject Maleimide Activated BSA and OVA* (n.d.): n. pag.

[47] O'Donoghue, Anthony J., A. Alegra Eroy-Reveles, Giselle M. Knudsen, Jessica Ingram, Min Zhou, Jacob B. Statnekov, Alexander L. Greninger, Daniel R. Hostetter, Gang Qu, David A. Maltby, Marc O. Anderson, Joseph L. DeRisi, James H. McKerrow, Alma L. Burlingame, and Charles S. Craik. "Global Identification of Peptidase Specificity by Multiplex Substrate Profiling." *Nature Methods*. U.S. National Library of Medicine, Nov. 2012.

[48] C. Southan, *FEBS Lett.*, 2001, 498, 214–218.

[49] López-Otín, Carlos, and Judith S. Bond. "Proteases: Multifunctional Enzymes in Life and Disease." *The Journal of Biological Chemistry*. American Society for Biochemistry and Molecular Biology, 07 Nov. 2008.

[50] Tamir, Ayala, Anju Gangadharan, Sakshi Balwani, Takemi Tanaka, Ushma Patel, Ahmed Hassan, Stephanie Benke, Agnieszka Agas, Joseph D'Agostino, Dayoung Shin, Sunghoon Yoon, Andre Goy, Andrew Pecora, and K. Stephen Suh. "The Serine Protease Prostate (PRSS8) Is a Potential Biomarker for Early Detection of Ovarian Cancer." *Journal of Ovarian Research*. BioMed Central, 2016.

[51] Tamir, Ayala, Anju Gangadharan, Sakshi Balwani, Takemi Tanaka, Ushma Patel, Ahmed Hassan, Stephanie Benke, Agnieszka Agas, Joseph D'Agostino, Dayoung Shin, Sunghoon Yoon, Andre Goy, Andrew Pecora, and K. Stephen Suh. "The Serine Protease Prostate (PRSS8) Is a Potential Biomarker for Early Detection of Ovarian Cancer." *Journal of Ovarian Research*. BioMed Central, 2016.

[52] Kaman, Wendy E., Fabiano Galassi, Johannes J. De Soet, Sergio Bizzarro, Bruno G. Loos, Enno C. I. Veerman, Alex Van Belkum, John P. Hays, and Floris J. Bikker. "Highly Specific Protease-Based Approach for Detection of *Porphyromonas Gingivalis* in Diagnosis of Periodontitis." *Journal of Clinical Microbiology*. American Society for Microbiology, Jan. 2012.

- [53] A. Stangelberger, M. Margreiter, C. Seitz and B. Djavan, *The Journal of Men's Health & Gender*, 2007, 4, 233–244.
- [54] Kimmel, Joe R., and Emil L. Smith. "Crystalline papain I. Preparation, specificity, and activation." *Journal of Biological Chemistry* 207.2 (1954): 515-531.
- [55] "A Biosensor Based on Magnetoresistance Technology1." A Biosensor Based on Magnetoresistance Technology1 - ScienceDirect. N.p., n.d.
- [56] Wang, Joseph. "Survey and summary from DNA biosensors to gene chips." *Nucleic acids research* 28.16 (2000): 3011-3016.
- [57] Wei, Cheng-Wey. "Using a microfluidic device for 1 μ l DNA microarray hybridization in 500 s." *Nucleic acids research* 33.8 (2005): e78-e78.
- [58] Gaster, Richard S. "Quantification of protein interactions and solution transport using high-density GMR sensor arrays." *Nature nanotechnology* 6.5 (2011): 314-320.
- [59] Osterfeld, Sebastian J. "Multiplex protein assays based on real-time magnetic nanotag sensing." *Proceedings of the National Academy of Sciences* 105.52 (2008): 20637-20640.
- [60] Rizzi, Giovanni. "Denaturation strategies for detection of double stranded PCR products on GMR magnetic biosensor array." *Biosensors and Bioelectronics* 93 (2017): 155-160.
- [61] Drew A. Hall, "GMR Spin-Valve Biochips and Interface Electronics for Ultrasensitive in-vitro Diagnostics," Ph.D. Thesis, Stanford University, 2011.
- [62] Wang, Shan X. "Analyte detection with magnetic sensors." U.S. Patent Application No. 12/234,506.
- [63] Wang, Shan X., and Guanxiong Li. "Advances in giant magnetoresistance biosensors with magnetic nanoparticle tags: review and outlook." *IEEE transactions on Magnetics* 44.7 (2008): 1687-1702.
- [64] Osterfeld, Sebastian J., and Shan X. Wang. "MagArray biochips for protein and DNA detection with magnetic nanotags: design, experiment, and signal-to-noise ratio." *Microarrays*. Springer New York, 2009. 299-314.
- [65] "Streptavidin MicroBeads." Miltenyi Biotec. N.p., n.d.
- [66] S. J. Osterfeld, H. Yu, R. S. Gaster, S. Caramuta, L. Xu, S.-J. Han, D. A. Hall, R. J. Wilson, S. Sun, R. L. White, R. W. Davis, N. Pourmand, and S. X. Wang, "Multiplex protein assays based on real-time magnetic nanotag sensing,"

Proceedings of the National Academy of Sciences, vol. 105, no. 52, pp. 20637-20640, Dec. 2008.

[67] S. J. Osterfeld, "A Microfluidic Biochip Based on Magnetoresistive Detection of Nanoparticles," Ph.D. dissertation, Dept. of Materials Science and Engineering, Stanford University, 2009.